

52
СИБИРСКОЕ ОТДЕЛЕНИЕ АН СССР
ИНСТИТУТ ЯДЕРНОЙ ФИЗИКИ

F.M.Izrailev

NEARLY LINEAR MAPPINGS AND THEIR
APPLICATIONS

ПРЕПРИНТ 80-149



Новосибирск

NEARLY LINEAR MAPPINGS AND THEIR
APPLICATIONS

F.M. Izrailev

Institute of Nuclear Physics
630090, Novosibirsk 90, USSR

A b s t r a c t

Simple 2-dimensional mapping is considered, both analytically and numerically, for which all nonlinear effects are of the order of perturbations and of the same origin. Peculiarities of the stochastic instability are exposed taking the beam-beam interaction in a storage ring as an important particular example of a dynamic system modelling by such mappings. A special case of time-dependent mappings is discussed. It is shown that low-frequency time dependence sharply cuts down the critical perturbation strength for the stochastic transition.

§1. INTRODUCTION

An efficient way to study physical processes is to construct an appropriate mathematical model. Such a model must retain the main properties of the phenomenon under study and must describe, at least qualitatively, the behavior of the real system. At the same time, it is certainly highly desirable to have a model that's simple enough to perform the theoretical analysis. In a sense, the so-called "mapping" may be considered to be one of the simplest examples of such a model. Various mappings have recently attracted wide attention (see, e.g., Ref. /1-2/). This attention is motivated by the understanding that the simplicity of a mapping does not necessarily imply simplicity of the system's behavior. Consider, for example, the mapping which seems to be by now the most thoroughly studied (see Ref. /3-7/):

$$\begin{aligned} p_{t+1} &= p_t + k_0 \sin x_t \\ x_{t+1} &= x_t + p_{t+1} \end{aligned} \quad (1.1)$$

Here p and x stand for the momenta and coordinates (or the "action-angle" variables); k_0 is the only model parameter that characterizes the perturbation strength. The difference equations (1.1) describe a nonlinear oscillator under the influence of an external kicks-like force. The same mapping is used to describe the motion of a charged particle in a magnetic trap /8/, the particle-wave interaction in a plasma /9/, etc. (see review article /7/). Furthermore, the mapping (1.1) models the motion near a nonlinear resonance in any arbitrary oscillating system. For this reason it was called the "standard mapping" /7/.

A study of mapping (1.1) has shown that the motion of this system is largely dependent upon the strength parameter k_0 . For example, for $k_0 \ll 1$ the oscillation is stable, while for $k_0 \gg 1$, there arises a new type of motion usually

called stochastic. Moreover, the motion in the latter case looks chaotic. This fact, striking at the first glance, is related to a strong instability of the motion that leads to a rapid mixing of trajectories in the phase space and to the appearance of statistical properties. A thorough numerical study reported in Ref. /7/ has proven that for $k_0 \gg 1$ the motion is completely governed by statistical laws. In the intermediate region, for $k_0 \sim 1$, the behavior of system (1.1) depends sensitively on the initial conditions and cannot be described in any simple manner (see Ref. /10/). Such systems were called "systems with divided phase space" /11/. The area preserving mapping (1.1) is a particular example of a Hamiltonian system with a nonlinear perturbation which depends periodically on time. According to the semi-qualitative approach developed in Refs. /12-14, 11,7/, the interaction between nonlinear resonances plays a key role in the appearance of stochasticity in such oscillating systems. For perturbations smaller than the critical one, the interaction between resonances is weak and the motion is essentially stable. Under a sufficiently strong interaction, the nonlinear resonances overlap, thus creating in the phase space a region where the trajectory is irregular. Even though the analytical estimates of the critical perturbation in such systems based on the study of a single resonance /14,7/ are not rigorous, they turn out to be, nevertheless, very efficient for the analysis of certain systems (see reviews /7,11,14-16/). The derivation of such estimates is based mainly upon the investigation of the basic characteristics of the nonlinear resonance, such as the resonance width and the dependence of oscillation frequency on the energy. Quite unexpectedly, the estimates get simplified significantly if the unperturbed motion is nonlinear, i.e., the perturbation is weak as compared to the nonlinearity /7/. From this point of view systems with nonlinear unperturbed motion and a weak perturbation seem to be the most convenient for analysis. If, on the contrary, all of the terms in the Hamiltonian, that represent the nonlinearity and the perturbation of the

system, are comparable in order of magnitude, this results in a nonlinear motion peculiarity and, consequently, the analytical consideration becomes rather complicated. Nevertheless, there are many important examples when an unperturbed motion represents linear oscillations and the nonlinearity arises only when a weak perturbation is involved. The mappings which describe such systems will be called "nearly linear" mappings.

It should be mentioned that nearly linear systems are typical for the asymptotic theory of nonlinear oscillations. This is the very case when the method of asymptotic expansion in a small parameter provides solutions for a number of problems in nonlinear mechanics (see, e.g., Ref. /17/). However, the most striking phenomenon - stochastic motion in the dynamic system - has not been found. As is clear now, the stochasticity is caused by the specific interaction of nonlinear resonances which was not considered previously in the traditional theory of nonlinear oscillations.

In this paper we consider the main properties of a particular nearly linear mapping. The main objective is to study the conditions necessary for the appearance of stochasticity. The interaction of colliding beams in a storage ring is taken as a model. In the simplest case, when one beam is far weaker than the other, the interaction between particles in the weak beam can be neglected. The problem is thus reduced to the study of repeated interactions of a single particle with a fixed strong beam (see, e.g., Ref. /18/).

§2. THE BASIC MAPPING

The simplest model of the periodic interaction of a single particle with a beam in storage ring can be described by the following equation :

$$x'' + K(s)x = f(x)\delta_t(s) \quad (2.1)$$

where x is the transverse displacement, $x' \equiv p = \frac{dx}{ds}$ is the transverse momentum of a particle, s is the longitudinal coordinate, and $\delta_L(s)$ is the periodic delta-function of a period L . The nonlinear function $f(x)$ is determined by the change of the particle's transverse momentum due to the interaction with the electro-magnetic field of the beam (see Refs. /18-19/). For simplicity we will call quantity $f(x)$ the force. The rigidity $K(s)$ is produced by the structure of the focusing magnetic field in the storage ring and, generally, depends upon s . As is seen from (2.1), only one-degree of freedom motion is considered without any connection to the motion on the other transverse coordinate. The model (2.1) means that the particle-beam interaction is assumed to be point-like. The latter assumption is valid only when the beam is bunched and the bunch is sufficiently short along the longitudinal coordinate s /18/.

In storage rings, the dependence $K(s)$ is periodic. For simplicity we assume that its period is equal to that of the external perturbation. Consequently, $L = L_0/m_0$, where m_0 is the number of interaction points over the ring, L_0 is the length of a closed orbit for the particle with zero transverse energy.

Thus (2.1) is a nonlinear equation with coefficients periodically dependent on the "time" s . Consider, first, the motion between kicks :

$$x'' + K(s)x = 0 \quad K(s+L) = K(s) \quad (2.2)$$

Using the Floquets theorem /20/, the general solution can be represented as the sum of two particular independent solutions :

$$x_{1,2}(s) = y_{1,2}(s)e^{\pm i\mu s/L}; \quad y_{1,2}(s+L) = y_{1,2}(s); \quad \mu = \text{const} \quad (2.3)$$

Therefore, it is convenient to look for $x(s)$ in the form /21/:

$$x_{1,2}(s) = A\beta^{1/2}(s)e^{\pm i\Phi(s)} \quad (2.4)$$

where the new function $\beta(s+L) = \beta(s)$ is introduced. The relation between $\beta(s)$ and $\Phi(s)$ can be derived from the Wronskian constancy conditions :

$$\beta(s)\Phi'(s) = \text{const} \quad (2.5)$$

The function $\beta(s)$, known in the theory of accelerators as the β -function (see Refs. /18,22-23/), has an obvious physical meaning. According to (2.4), it determines the instantaneous amplitude of transverse (betatron) oscillations : $x_m(s) \sim \beta^{1/2}(s)$. The square root of the β -function actually gives the envelope of the betatron oscillations along the longitudinal coordinate. From Eg.(2.3-2.5) we obtain

$$\mu = \int_s^{s+L} ds/\beta(s) \quad (2.6)$$

It means that parameter μ is the betatron phase advance between two neighboring interaction points. We may now introduce the dimensionless frequency of transverse oscillations averaged over the revolution period (the so-called tune) :

$$\nu = \frac{m_0\mu}{2\pi} = \frac{1}{2\pi} \int_s^{s+L_0} ds/\beta(s)$$

For $\beta = \text{const}$ we have $\nu = L_0/2\pi\beta = R/\beta$, where R is the mean radius of the particle equilibrium orbit /23/.

Substituting (2.4) into (2.2) we find the relation between the β -function and $K(s)$:

$$\frac{1}{2} \beta\beta'' - \frac{1}{4} \beta'^2 + K(s)\beta^2 = 1 \quad (2.7)$$

Hence, the solution of (2.2) can be obtained once the dependence $\beta(s)$ is known. The result is

$$x(s) = A\beta^{1/2}(s)\cos\left[\int_0^s \frac{ds}{\beta(s)} + \Phi_0\right] + B\beta^{1/2}(s)\sin\left[\int_0^s \frac{ds}{\beta(s)} + \Phi_0\right] \quad (2.8)$$

From (2.8) the mapping for (x, p) in the period L can be readily obtained

$$p_{t+1} = -\frac{\sin \mu}{\beta} \left[1 + \frac{1}{4} \beta'^2\right] x_t + \left[\cos \mu + \frac{1}{2} \beta' \sin \mu\right] p_t \quad (2.9)$$

$$x_{t+1} = (\cos \mu - \frac{1}{2} \beta' \sin \mu) x_t + \beta p_t \sin \mu$$

The mapping (2.9) is almost equivalent to eg. (2.2) the only exception being that it gives solutions only for certain particular values $s=s_L$. Since (2.9) are given in the form of difference equations, their numerical simulation appears to be much simpler than that of (2.2). To iterate (2.9), it is sufficient to know μ and the value of the β -function and its derivative $\beta'(s)$ at the interaction points $s=s_L$. The time is measured in number of iterations (2.9). Certainly, reducing the difference equation (2.2) to mapping (2.9) makes sense only when the values $\beta(s_L)$ and $\beta'(s_L)$ are known. This is the case in storage rings for which $\beta(s)$ is determined by the given magnetic structure of the facilities.

To obtain the total mapping for system (2.1), the influence of the particle-beam interaction must be taken into account. Since the perturbation is assumed to be point-like, it effects only momentum

$$\begin{aligned} \bar{p} &= p + f(x) \\ \bar{x} &= x \end{aligned} \quad (2.10)$$

Here the values of (\bar{p}, \bar{x}) after a kick are expressed via values (p, x) before the kick. Since in the interaction points $\beta'(s_L)=0$, the total mapping for one period is :

$$\begin{aligned} p_{t+1} &= -\frac{x_t}{\beta} \sin \mu + p_t \cos \mu + f(x_t) \cos \mu \\ x_{t+1} &= x_t \cos \mu + \beta p_t \sin \mu + \beta f(x_t) \sin \mu \end{aligned} \quad (2.11)$$

The same equations can be used to describe an oscillator with a constant frequency $K=\text{const}$ and $\beta=1/\sqrt{K}$. Therefore, mapping (2.11) may be regarded as a general model of a linear oscillator with frequency $\omega_0=1/\beta$ under the nonlinear force in the form of periodic δ -function kicks.

Numerous analytical and numerical studies of mapping (2.11) have been performed (see, e.g., Refs. /1,3,24-33/). Although this mapping seems to be highly specific, it is actually of a rather general type. This becomes evident when the mapping (2.11) is rewritten in another form :

$$x_{t+1} + x_{t-1} = c_0 x_t + d_0 f(x_t) \quad (2.12)$$

where $c_0=2 \cos \mu$, $d_0=\beta \sin \mu$. Equation (2.12) is a difference equation of the second order and has many applications. Specifically, it is used in the theory of difference schemes (see, e.g., Ref. /34/).

As mentioned above, in general, there is no rigorous theory that could provide the answer for the main question : under which conditions is the motion described by (2.12) stochastic? Therefore, the semi-qualitative approach developed in Refs. /12,14,7/ is the only way to derive analytical estimates of the stochasticity criterion. Let us choose the force $f(x)$ as (see Fig.1) :

$$f(x) = -\frac{4\pi\xi}{\beta} x \frac{1-\exp(-x^2/2\sigma^2)}{x^2/2\sigma^2} \quad (2.13)$$

This force corresponds to a "round" beam with a Gaussian transverse charge distribution which depends only on the displacement x from the central orbit. In (2.13) σ is the mean square root of the transverse size of the beam ; β is the β -function at the interaction points. The parameter $\xi > 0$ determines the interaction strength and is proportional to the beam current. The negative sign corresponds to the interaction of opposite charges.

Substituting (2.13) into (2.11) and introducing the dimensionless variables $X = x/\sigma$, $P = \beta \cdot p/\sigma$, we get the basic mapping :

$$P_{t+1} = -X_t \sin \mu + P_t \cos \mu + F(X_t) \cos \mu \quad (2.14)$$

$$X_{t+1} = X_t \cos \mu + P_t \sin \mu + F(X_t) \sin \mu$$

$$F(X) = -4\pi\xi X_t \frac{1 - \exp(-X^2/2)}{X^2/2}$$

Note that the mapping (2.14) depends only upon the two parameters, ξ and μ .

Consider, first of all, the motion for small $X \ll 1$ for which the force $F(X)$ is linear. The condition for the stability of small oscillations can be readily obtained from (2.14) /30/ :

$$-2\text{ctg } \mu/2 < -4\pi\xi < 2\text{tg } \mu/2 \quad \text{for } \sin \mu > 0 \quad (2.15)$$

$$2\text{tg } \mu/2 < -4\pi\xi < -2\text{ctg } \mu/2 \quad \text{for } \sin \mu < 0$$

As is seen from Fig. 2, the main region of linear stability is above the parametric resonance given by $\mu/\pi = k$, with k an integer. Condition (2.15) repeats in μ with a period $\Delta\mu = \pi$. As follows from (2.14), for the total nonlinear mapping (2.14) the period also equals $\Delta\mu = \pi$. This is due to the asymmetry of the force $F(X)$ with respect to $X = 0$. In general, $\Delta\mu = 2\pi$ (see §5). Outside the shaded area in Fig. 2, the small oscillations are unstable and the amplitude is restricted only by the nonlinearity (see §3).

If the force $f(x)$ is linear everywhere, the mapping (2.11) is exactly equivalent to the Hill equation with the frequency dependence on time given by the periodic δ -function :

$$x'' + \omega_0^2 x = -A_0 x \delta_L(s) \quad (2.16)$$

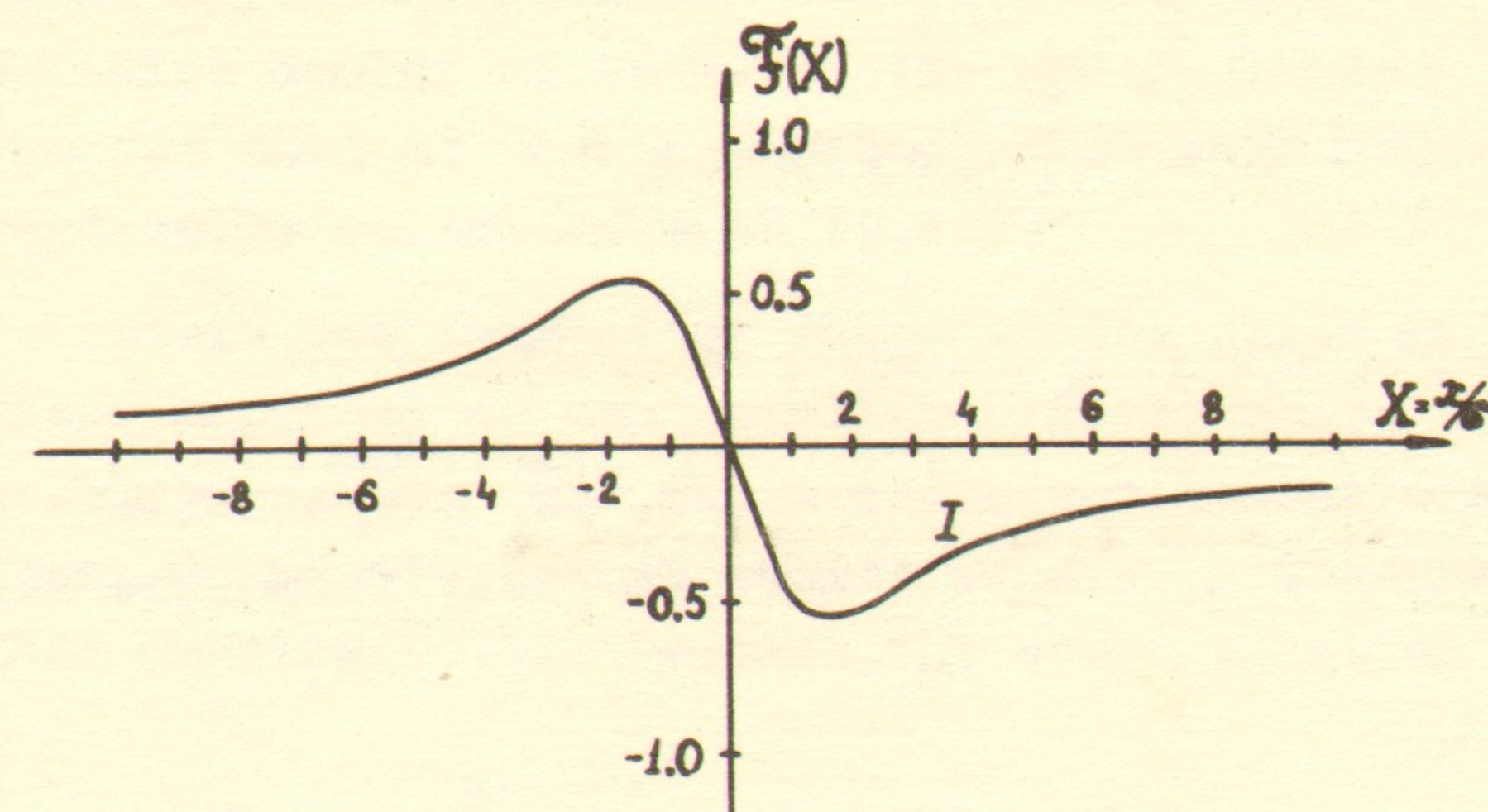


Fig. 1. The dependence F (2.13) on the dimensionless displacement $X = x/\sigma$ for normalized parameters $8\pi\xi/\beta = 1$.

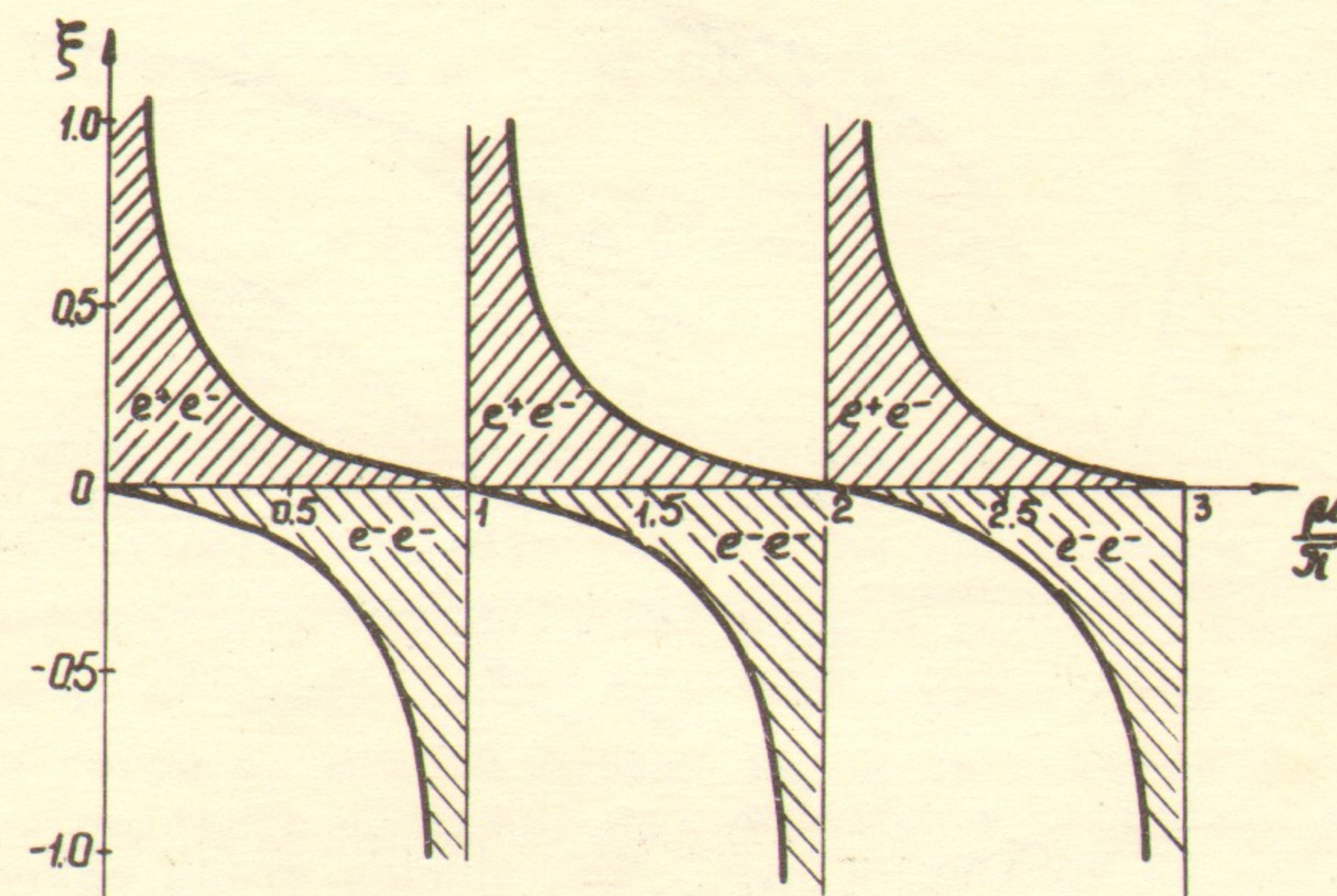


Fig. 2. The stability condition (shaded areas) for small oscillations (2.15). The values $\xi < 0$ and $\xi > 0$ correspond to the interaction of the same and opposite charges, respectively.

where $\delta_L(s) = \frac{1}{L} (1 + 2 \sum_{l=1}^{\infty} \cos l \frac{2\pi s}{L})$. We now rewrite ω_0, A_0 in terms of ξ, v and reduce (2.16) to the usual form:

$$x'' + (b - 2q \sum_{l=1}^{\infty} \cos l \Omega s) x = 0 \quad (2.17)$$

$$b^2 = v^2 + 4\xi v; \quad q = -4\xi v; \quad \Omega = \frac{2\pi v}{\mu}$$

In the standard variables $-2q/b, \sqrt{b}$ the stability areas (2.14) shown in Fig. 2 have a more familiar form (see Fig. 3).

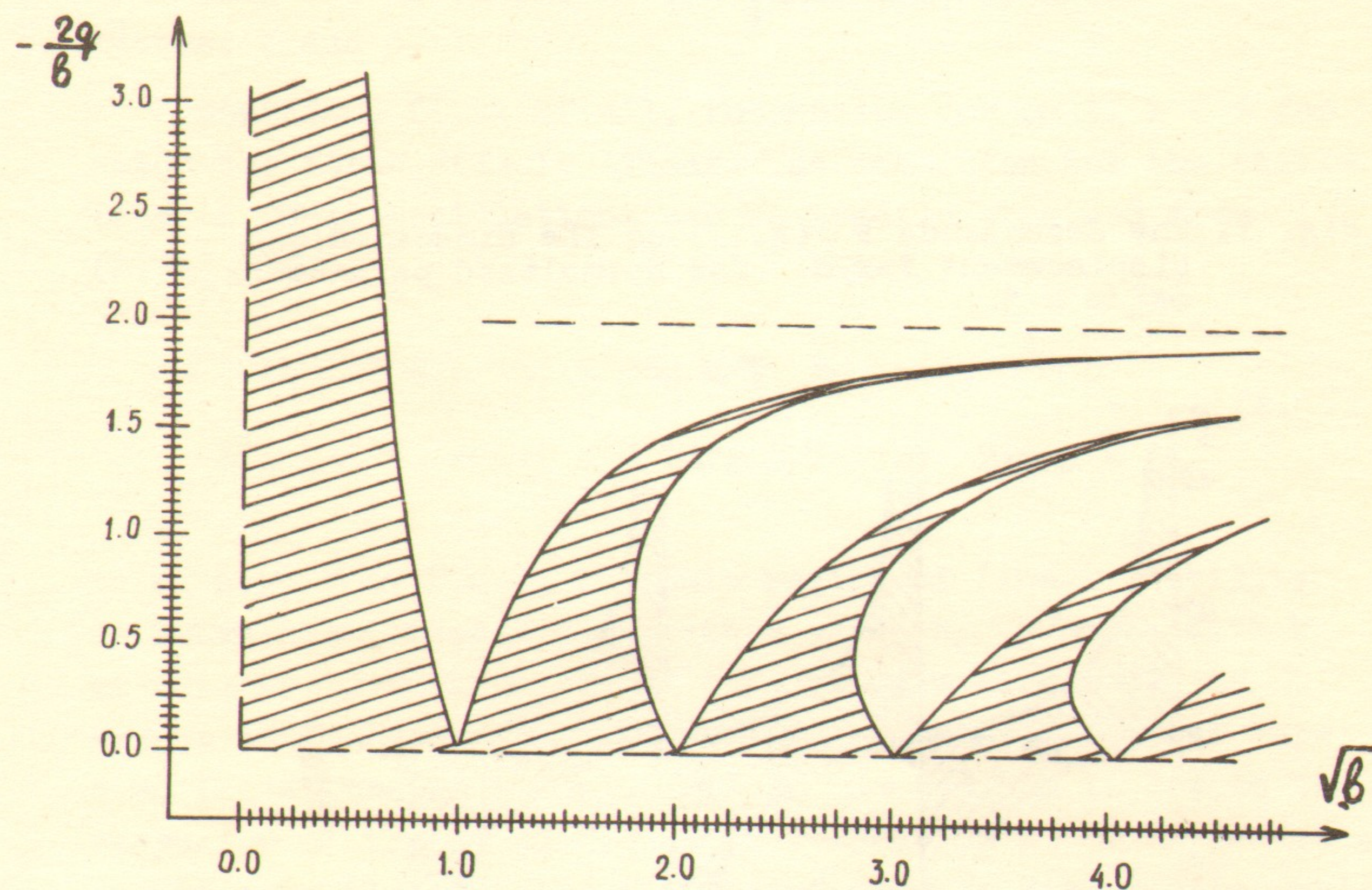


Fig. 3. The stability condition for the Hill equation (2.17) in variables q, b . The shaded areas correspond to those in Fig. 2 for $\xi > 0$. The left lines of each stable zone are described by the simple analytical form: $-2q/b = 2(1 - v_k^2/b)$, where $\sqrt{b} \geq v_k = m_0 k/2$. These lines correspond to the vertical lines in Fig. 2. The dotted horizontal line denotes the limit value of $-2q/b$ which equals $-2q/b = 2$. This is the case of two interaction points: $m_0 = 2$.

Note that the analytical expression for the stability borders is in good agreement with the numerical results /35/ in which only a finite number of terms in the sum $\sum_{l=1}^M \cos l \Omega s$ were taken. It turns out that at $M \geq 5$ the border already changes slightly and practically coincides with (2.14).

To obtain the trajectory shape in the phase (x, p) for the linear mapping, we use equations (2.11) where the force is linear: $f(x) = -\frac{4\pi\xi}{\beta} x$. One can perform the linear transformation from (x, p) to new variables (x^*, p^*) in such a way that the mapping (2.11) becomes the usual rotation

$$p_{t+1}^* = -\frac{1}{\beta^*} x_t^* \sin \mu^* + p_t^* \cos \mu^* \quad (2.18)$$

$$x_{t+1}^* = x_t^* \cos \mu^* + \beta^* p_t^* \sin \mu^*$$

The new parameters μ^*, β^* are related to the previous ones by the following relations /21/:

$$\cos \mu^* = \cos \mu - 2\pi\xi \sin \mu; \quad \beta^* \sin \mu^* = \beta \sin \mu \quad (2.19)$$

$$\beta = \beta^* \sqrt{1 - 4\pi^2 \xi^2 + 4\pi\xi \operatorname{Ctg} \mu}$$

where only two of them are independent.

The stable trajectories in the phase space described by mapping (2.18) are elliptical with a ratio of maximal sizes in p^* and x^* equal to $p_m^*/x_m^* = 1/\beta^*$. Hence, the influence of the linear force on stable motion leads to a stretching of the phase ellipse by a factor of β/β^* along p and to a shift in angle equal to $\mu/2$ in variables (X, P) . The stability condition (2.15) in the new variables becomes very simple: $|\cos \mu^*| < 1$.

We can see from relations (2.19) that for small ξ the value μ changes slightly ($\Delta\mu = \mu^* - \mu \ll \mu$). This change equals approximately $\Delta\mu = 2\pi\xi$. Since $\mu = 2\pi v/m_0$, this means that the change in the oscillation frequencies is also proportional to

ξ and equals $\Delta v = m_0 \xi$. This is the linear tune shift caused by the particle-beam interaction. This shift is proportional to the beam current and to the number of interaction points in the storage ring.

However, the above expression for Δv is only valid far away from the parametric resonance, when $\Delta\mu \ll 2\pi\delta_1$ with $\delta_1 = \{\mu/\pi\}$ (the braces denote the fractional part). An exact expression for $\Delta\mu$ is derived from the relations (2.19): $\Delta\mu = \arccos(\cos\mu - 2\pi\xi\sin\mu) - \mu$. In the limit case, in the vicinity of the parametric resonance and above it, we have: $\text{tg } \Delta\mu \approx 2\pi\sqrt{\delta_1\xi}$. Therefore, if $\delta_1 \ll 1/4\pi^2\xi$ the tune shift can be significantly smaller than $m_0\xi$. In this case $\Delta v = m_0\sqrt{\delta_1\xi}$. The phase ellipse slightly above the parametric resonance is strongly stretched with

$$\frac{p_m^*}{x_m^*} \approx 2\sqrt{\frac{\xi}{\delta_1}}$$

This means that the transverse momentum at the interaction points becomes very large.

Now we consider the particle motion which is not restricted to the linear approximation. For this purpose we write an exact Hamiltonian corresponding to equation (2.1):

$$H = \frac{p^2 + K(s)x^2}{2} + V(x)\delta_L(s); \quad V(x) = -\int f(x)dx \quad (2.20)$$

Using the generating function

$$F_1(x, \Psi) = \frac{x^2}{2\beta} \text{tg} \left[\Psi - \frac{vs}{2\pi L_0} + \int_0^s \frac{ds}{\beta} \right] + \frac{x^2}{4\beta} \beta'; \quad \beta = \beta(s) \quad (2.21)$$

we carry out the canonical transformation to "action-angle" variables /36/:

$$x = \sqrt{2J\beta} \cos \left[\Psi - \frac{vs}{2\pi L_0} + \int_0^s \frac{ds}{\beta} \right] \quad (2.22)$$

$$p = \sqrt{\frac{2J}{\beta}} \sin \left[\Psi - \frac{vs}{2\pi L_0} + \int_0^s \frac{ds}{\beta} \right] + \frac{\beta'}{2} \sqrt{\frac{2J}{\beta}} \cos \left[\Psi - \frac{vs}{2\pi L_0} + \int_0^s \frac{ds}{\beta} \right]$$

In the variables (J, Ψ) the new Hamiltonian is

$$H = Jv + V(J, \Psi)\delta_T(\Theta) \quad (2.23)$$

where s has been replaced by a new dimensionless variable $\Theta = 2\pi s/L_0$. The kick period equals $T = 2\pi/m_0$.

If the values of β - function in (2.1) are the same and $\beta'(s) = 0$ at the interaction points $s = s_L$ the potential in (2.23) is independent on Θ . Then the relation between (x, p) and (J, Ψ) for these points becomes the usual:

$$x = \sqrt{2J\beta(s_L)} \cos \Psi; \quad p = \sqrt{\frac{2J}{\beta(s_L)}} \sin \Psi \quad (2.24)$$

The peculiarity of the model Hamiltonian (2.20) is that the nonlinearity is caused only by the perturbation. This fact complicates the study of the stochasticity criterion. Nevertheless, the general approach based on the investigation nonlinear resonances appears to be very fruitful in this case as well.

§ 3. The Simple Resonance Approximation

The potential of the particle-beam interaction for the force (2.13) can be written as

$$V(J, \Psi) = \frac{4\pi\xi}{\beta} \sigma^2 \int_0^1 \frac{1 - e^{-2v\eta}}{\eta} d\eta \quad (3.1)$$

where

$$v = a \cdot \cos^2 \Psi; \quad a = \frac{J\beta}{2\sigma^2} = \left[\frac{x_m}{2\sigma} \right]^2 \quad (3.2)$$

Here x_m is the maximum value of the particle displacement; $2a$ is the transverse energy. Since the perturbation is assumed

to be small, it seems natural to extract the most essential resonance terms. With this aim, we put $V(J, \Psi)$ and $\delta_T(\theta)$ into a Fourier series

$$V(J, \Psi) = \sum_{n=-\infty}^{+\infty} V_n(J) e^{-in\Psi}; \quad \delta_T(\theta) = \frac{m_0}{2\pi} \sum_{k=-\infty}^{+\infty} e^{ik\theta} \quad (3.3)$$

After a number of manipulations we arrive at

$$H = J\nu + \varepsilon \int_0^1 \frac{d\eta}{\eta} \left[1 - e^{-a\eta} \sum_{n=-\infty}^{+\infty} I_n(a\eta) e^{-2in\Psi} \right] \sum_{k=-\infty}^{+\infty} e^{ik\theta} \quad (3.4)$$

Here $I_n(a\eta)$ is the modified Bessel function of the n -th order, and ε is a new strength parameter, $\varepsilon = \frac{\xi}{\beta} m_0 2\sigma^2$.

In the approximation of the single resonance*, only the influence of the nearest resonance is considered. This is equivalent to the averaging of the perturbation over an unperturbed motion close to the single resonance under consideration. Consequently, in the Hamiltonian (3.4), beside the zeroth harmonic, there remain only those terms for which $2n\Psi - k\theta \approx 0$. In this case, taking into account the relation $\dot{\theta} = \Omega = 2\pi/T = m_0$ the resonance condition is

$$\Psi = \frac{m_0 k}{2n} \quad (3.5)$$

Due to the symmetry of $V(x)$ with respect to $x=0$, the Fourier expansion has only even harmonics $2n$. As a result of the nonlinear perturbation, the tune $\Psi = \nu + \Delta\nu$ depends upon the action J . Thus, for given k, n condition (3.5) is satisfied for only certain value of the transverse energy. Being affected by the resonance, the energy will increase and the system will move out of resonance. In this way, the nonlinear single resonance (in contrast to the linear one) stabilizes the motion. In order to find the dependence $\Delta\nu(J)$ it is convenient to single out from the perturbation the nonlinearity which is independent

* The single nonlinear resonance as applied to the theory of accelerators has been considered in detail in Refs. /37, 22, 38/.

of the phases Ψ and θ . Then the Hamiltonian (3.4) can be written as

$$H = J\nu + \varepsilon \int_0^1 \frac{d\eta}{\eta} \left\{ 1 - e^{-a\eta} I_0(a\eta) \right\} - \\ - 2\varepsilon \int_0^1 \frac{d\eta}{\eta} e^{-a\eta} \sum_{l_0=1}^{\infty} I_{nl_0}(a\eta) \cos l_0(2n\Psi - k\theta) \quad (3.6)$$

Summation over l_0 in (3.6) implies, generally, the necessity of taking into account all the resonance terms for which $l_0(2n\Psi - k\theta) \approx 0$. The contribution of the resonance terms with $l_0 \neq 1$ in our model can be rather significant /39/.

For further consideration it is convenient to transform to a new phase $\vartheta_{nk} = \Psi - \frac{k\theta}{2n}$, assuming the action J to be the same. Then the new Hamiltonian will not depend on the external phase θ . The generating function for this transformation is $F_2(J, \vartheta_{nk}, \theta) = -J \cdot (\vartheta_{nk} + \theta)$. In the new variables we obtain the resonance Hamiltonian which remains constant

$$H_{nk} = J\delta_{nk} + \varepsilon \int_0^1 \frac{d\eta}{\eta} \left\{ 1 - e^{-a\eta} I_0(a\eta) \right\} - \\ - 2\varepsilon \int_0^1 \frac{d\eta}{\eta} e^{-a\eta} \sum_{l_0=1}^{\infty} I_{nl_0}(a\eta) \cos l_0 2n\vartheta_{nk} \quad (3.7)$$

where $\delta_{nk} = \nu - \frac{k\Omega}{2n}$ is the detuning from the resonance value of frequency. The motion equations in variables (J, ϑ_{nk}) are

$$\dot{\vartheta}_{nk} = \delta_{nk} + \Delta\nu(a) - 2m_0 \xi \frac{e^{-a}}{a} \sum_{l_0=1}^{\infty} I_{nl_0}(a) \cos 2nl_0 \vartheta_{nk} \quad (3.8)$$

$$\dot{J} = -4m_0 \xi n \sum_{l_0=1}^{\infty} \int_0^1 \frac{d\eta}{\eta} e^{-a\eta} I_{nl_0}(a\eta) \sin 2nl_0 \vartheta_{nk}$$

The first equation in (3.8) describes the slow change of a new phase ϑ_{nk} , which can either change infinitely or oscillate

around a resonance value. The last case of phase oscillation is just the case of the nonlinear resonance [7]. It is clear that when the sum in eq. (3.8) for δ_{nk} is sufficiently small, the frequency of the phase oscillations can be readily obtained: $\omega_{ph} = \dot{\vartheta}_{nk} = \delta_{nk} + \Delta v(a)$. In the same approximation $\Delta v(a)$ yields a nonlinear tune shift which depends upon the transverse energy of a particle:

$$\Delta v(a) = \frac{m_0 \xi}{a} \left[1 - e^{-a} I_0(a) \right] \quad (3.9)$$

For $a \ll 1$ from (3.9) we obtain a result $\Delta v = m_0 \xi$ which we recognize to be the same as that in § 2. In another limit case, for $a \gg 1$ the tune shift is inversely proportional to the energy: $\Delta v = m_0 \xi / a$ (see Fig. 4). As will be shown below,

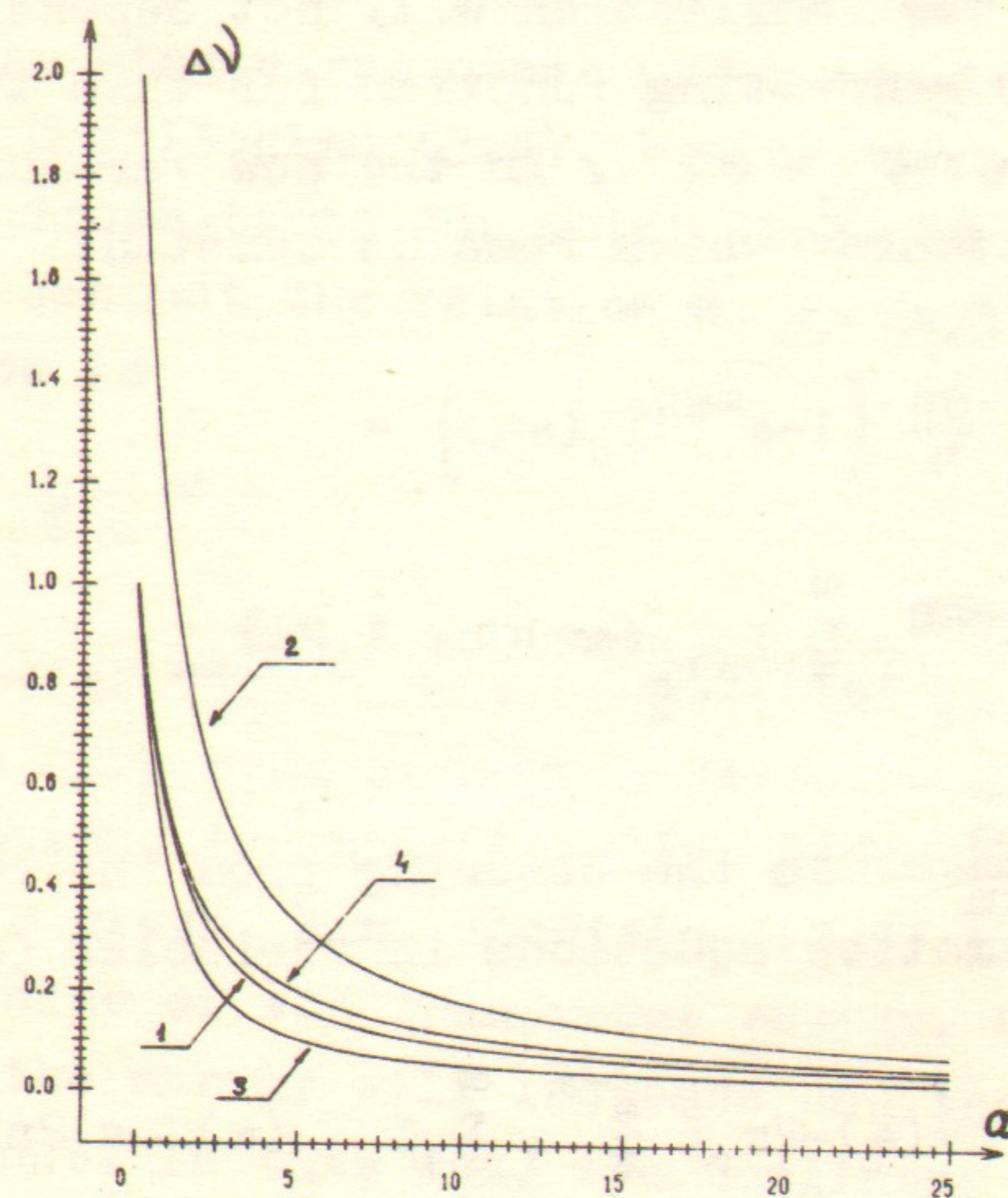


Fig. 4. The nonlinear shift dependence Δv on a (a is a half transverse energy of the particle). Curve I represents the mean tune shift for linear oscillations (3.9). Curve II is the maximal tune shift for the parametric resonance $n=1$ (3.12); curves III and IV are the same for the low-order resonances $n=2$ and $n=3$ respectively (at the phase $\vartheta = \pi/2$).

the nonlinear dependence $\Delta v(a)$ is one of the most important characteristics of nonlinear resonances.

Since the tune shift $\Delta v(a)$ is proportional to the strength parameter ξ it follows from eq. (3.7) that (3.9) is valid when the sum $\sum_{l_0=-\infty}^{\infty} I_{n l_0}(a)$ is small. Clearly, for small n this condition is not fulfilled. Consider, for example, a parametric resonance: $n=1$ (it is equivalent to $\mu/\pi=k$ or $v=m_0 k/2$, see § 2). It is necessary then to take into account all the terms in the sum, since for moderate values of a terms $I_{l_0}(a)$ decrease slowly with respect to l_0 . Now it seems more convenient to rewrite the Hamiltonian (3.7) as

$$H_k = J \delta_1 + \varepsilon \int_0^1 \frac{d\eta}{\eta} \left\{ 1 - e^{-a\eta} \sum_{l_0=-\infty}^{\infty} I_{l_0}(a\eta) \cos 2l_0 \vartheta_k \right\} \quad (3.10)$$

The motion equations for J, ϑ_k are

$$\begin{aligned} \dot{\vartheta}_k &= \delta_1 + \Delta v_1(a, \vartheta_k); \quad \Delta v_1(a, \vartheta_k) = \frac{m_0 \xi}{a} \left\{ 1 - e^{-a} \sum_{l_0=-\infty}^{+\infty} I_{l_0}(a) \cos 2l_0 \vartheta_k \right\} \\ \dot{J} &= -2\varepsilon \int_0^1 \frac{d\eta}{\eta} e^{-a\eta} \sum_{l_0=-\infty}^{+\infty} l_0 I_{l_0}(a\eta) \sin 2l_0 \vartheta_k \end{aligned} \quad (3.11)$$

From (3.11) we can easily find the fixed points ϑ_k^0, J^0 which satisfy the condition $\dot{\vartheta}_k = \dot{J} = 0$. From the second equation in (3.11) we obtain $\vartheta_k^0 = 0, \pm \pi/2, \pm \pi, \dots$. Since the maximum value of the sum in the first eq. (3.11) equals $\sum_{l_0=-\infty}^{+\infty} I_{l_0}(a) = e^a$, for $\delta_1 > 0$ there are no fixed points. It means that above the parametric resonance, for $v > m_0 k/2$ the phase oscillations are absent. If $\delta_1 < 0$ the zero point $\vartheta_k^0 = J^0 = 0$ is a stable fixed point under the condition $m_0 \xi < \delta_1/2$. The latter relation coincides with the criterion of linear stability (2.15). If, alternatively, $m_0 \xi > \delta_1/2$ the zero point becomes unstable and another stable fixed point appears. Its location is defined by the relations:

$$\vartheta_k^{(1)} = \pm \frac{\pi}{2}; |\delta_1| = \frac{4m_0\xi}{a_1} e^{-a_1} \sum_{l=0}^{\infty} I_{2l+1}(a_1) = \Delta v_1(a_1) \quad (3.12)$$

In this case the region of the nonlinear parametric resonance can be found from the Hamiltonian (3.10). The qualitative representation of this region is given in Fig. 5. The separatrix

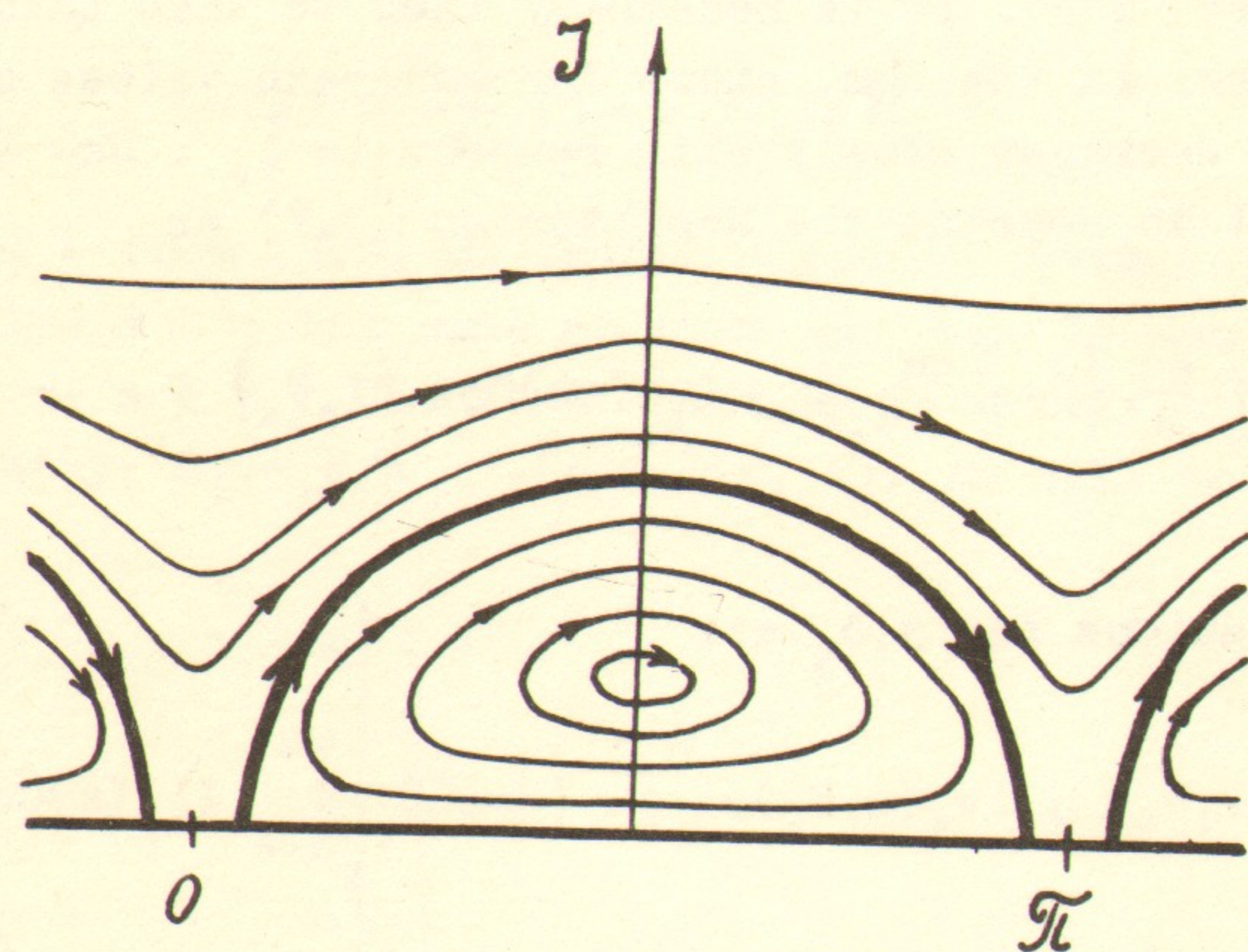


Fig. 5. The qualitative representation of the phase trajectories near the parametric resonance in J and ϑ_k variables. A thick line is the separatrix.

trix that divides the oscillation and phase rotation regions lies partly on the axis $J=0$. From (3.11) it is seen that the transverse energy can drastically change slightly below the parametric resonance. This creates strong oscillations of the nonlinear tune shift $\Delta v_1(a)$ around a mean value, which, in general, can significantly differ from (3.9). For example, at exact resonance ($\vartheta = \pi/2$, $a = a_1$) a mean value is derived from (3.12). The maximum tune shift is reached for $a \ll 1$ and equals $(\Delta v_1)_{\max} = 2m_0\xi$. This is two times higher than the mean tune shift for li-

near oscillations (3.9). Relation (3.12) for $\Delta v_1(a)$ (Fig. 4) describes not only the shift for the resonance value of energy $2a_1$ but also for any motion at the moment of the phase passing $\vartheta = \pi/2$ (see Fig. 5). We can compare the nonlinear shifts of other low resonances $n=2;3$ (at the same phase $\vartheta = \pi/2$). As is seen, (Fig. 4) for $n=3$ the expression (3.9) already appears to be a satisfactory approximation for $\Delta v(a)$.

Fig. 6 illustrates the phase plane (X,P) of mapping (2.14) for various initial values (X_0, P_0) [30]. Since $m_0=2$ and $\nu = 3.65$ for these calculations, the strongest resonances ac-

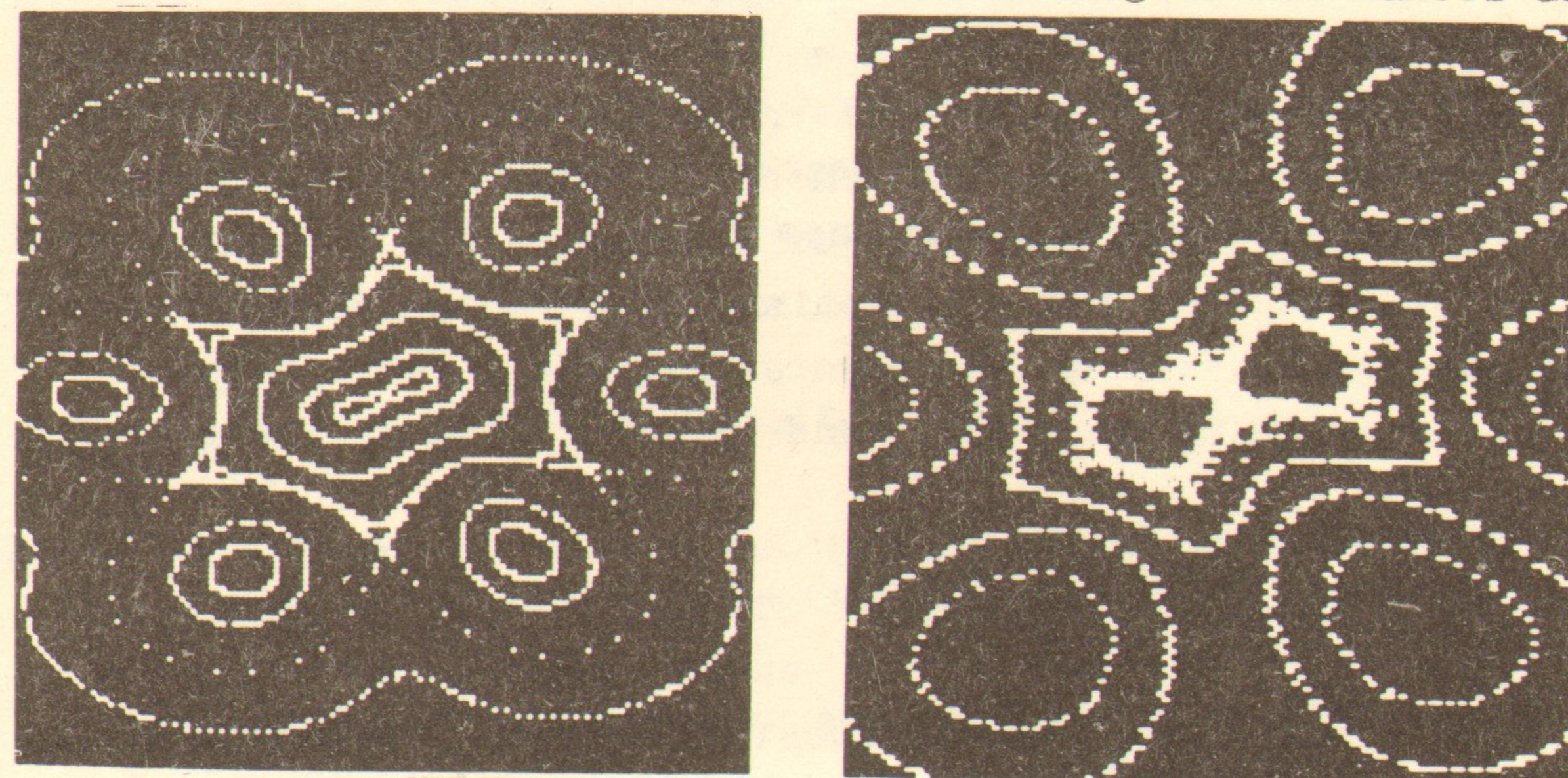


Fig. 6. The phase space structure for basic mapping (2.14) with $m_0=2$. The horizontal axis is the X - axis in the range $|X| \leq 10$; the vertical axis is the P - axis in the range $|P| \leq 15$. The center of the picture corresponds to $X = P = 0$. For each trajectory here and further the number of iterations (2.14) is $N=10^4$. The unperturbed tune equals $\nu = 3.65$. Fig. 6a - for $\xi = 0.12$; Fig. 6b - for $\xi = 0.24$.

ording to (3.5), are $2k/2n=2/3$ and $2k/2n=1$. For convenience, we neglect the integer part of ν . The resonance $2k/2n=3/4$ in Fig. 6a is not seen because, as will be shown below, the resonance strength drastically falls as n increased. The number of resonance regions for the chosen force (2.13) is always $2n$. The region of the parametric resonance is clearly seen near $X=P=0$ in Fig. 6 (see also Fig. 5). Also seen are the stable trajectories which surround the resonance at large trans-

verse energies.

The resonance value a_1 can be readily determined with a computer experiment by introducing a slight damping for the phase trajectory located inside the resonance region. The influence of this damping is such that the trajectory is attracted to the fixed points $(\pm X_1, \pm P_1)$ thus determining the coordinates of these latter. If we know X_1, P_1 in the linear approximation the transverse energy may be estimated as $2a_1^0 = (X_1^2 + P_1^2)/2$. The values of a_1^0 are $a_1^0 \approx 0.29$ and $a_1^0 \approx 1.5$ for $\xi = 0.12$ (Fig. 5a) and for $\xi = 0.24$ (Fig. 5b), respectively. The analytical estimates obtained by (3.12) for $\xi = 0.12$ and 0.24 are $a_1 \approx 0.35$ and $a_1 \approx 1.3$ respectively. Differences in the numerical and analytical estimates of a_1 can be explained, for example, by the influence of strong resonance $2k/2n = 2/3$ (see Fig. 6b). The width of the parametric resonance in a is derived from the Hamiltonian (3.10) which remains constant and equals zero on the separatrix. The maximum value of a_m is reached at $\vartheta = \pm \pi/2$ and is determined by the relation

$$\delta_1 a_m = m_0 \xi \int_0^{a_m} \frac{d\eta}{\eta} \left\{ 1 - e^{-\eta} \left[I_0(\eta) + 2 \sum_{l=1}^{\infty} (-1)^l I_l(\eta) \right] \right\}$$

Using the data from Fig. 6a, the numerical integration gives $a_m \approx 0.7$. At the same time, a rough determination of a_m from this figure gives the value $a_m^0 \approx 0.5$. In Fig. 6b the separatrix of the parametric resonance for $\xi = 0.24$ appears to be destroyed. This is a result of the action of the neighbouring resonance $2k/2n = 3/4$ whose influence for a given value of ξ leads to the creation of a stochastic region close to the separatrix of the parametric resonance (see § 4). Nevertheless, the size of the separatrix ($a_m^0 \approx 4.4$) is in good agreement with the analytical estimate ($a_m \approx 4.0$)

For a given force (2.13) it is found that for $n \geq 3$ the sum in (3.8) is significantly less than the nonlinear shift $\Delta v(a)$. Therefore, an extraction of the nonlinearity in (3.7) becomes convenient in deriving analytical estimates. In this case, with respect to the extracted nonlinearity the remaining terms that

depend on the phase ϑ_{nk} can be considered a weak perturbation. The fact that for high resonances $n \gg 1$ the amplitude sharply decreases is associated with the analyticity of the function $f(x)$. Thus, although the mapping (2.14) is nearly linear, for $n \gg 1$ the problem is reduced to the case in which an unperturbed Hamiltonian is nonlinear and the perturbation is weak. The latter situation, as mentioned above, is simpler from the point of view of obtaining efficient estimates [7, 11, 14].

Consider now a high-order nonlinear resonance $n \gg 1$. The Hamiltonian (3.7) can now be written as:

$$H_{nk}(J, \vartheta_{nk}) = H_0(J) + \varepsilon V^0(J, \vartheta_{nk}) \quad (3.13)$$

where $H_0(J)$ is an unperturbed nonlinear Hamiltonian, and the perturbation εV^0 is weak compared to $H_0(J)$. This implies that the change ΔJ is small near the resonance value $J^{(nk)}$ which satisfies the relation

$$\delta_{nk} + \frac{m_0 \xi}{a_{nk}} \left\{ 1 - e^{-a_{nk}} I_0(a_{nk}) \right\} = 0; \quad J^{(n,k)} = \frac{a_{nk}}{\beta} 2\sigma^2 \quad (3.14)$$

It is convenient to perform another canonical transformation to a new action q , resulting in the change of the previous action J near the resonance value $J^{(n,k)}$ via $J = J^{(n,k)} + q$. The corresponding generating function is $F_3(J, \vartheta_{nk}, \theta) = -(J - J^{(n,k)}) \cdot (\vartheta_{nk} + \theta)$. Using new variables and taking a small value of $q \ll J^{(nk)}$ into account, the Hamiltonian (3.7, 3.13) becomes much simpler

$$H_n(q, \vartheta_{nk}) = \frac{q^2}{2} (\Delta v)_j^* + \varepsilon V^0(J^{(n,k)}, \vartheta_{nk}); \quad (\Delta v)_j^* \equiv \frac{\partial(\Delta v(a))}{\partial J} \quad (3.15)$$

$$\varepsilon V^0 = -2\varepsilon \sum_{l_0=1}^{\infty} \int_0^1 \frac{d\eta}{\eta} e^{-a\eta} I_{n l_0}(a\eta) \cos l_0 2n\vartheta_{nk}$$

where $(\Delta v)_j^*$ and V^0 are taken for the resonance value $J = J^{(n,k)}$. Eq. (3.15) was derived by using the expansion of the unperturbed Hamiltonian $H_0(J)$ in q up to terms in q^2 and by taking into account relation (3.14).

If in the perturbation $\varepsilon V^0(J^{(n,k)}, \vartheta_{nk})$ we keep only the first term of the sum (see (3.7)), then the Hamiltonian (3.15) will coincide with the Hamiltonian of a pendulum [7,14]:

$$H_{nk}(q, \vartheta_{nk}) = \frac{q^2}{2} (\Delta v)_j^2 + \varepsilon V_n^0 \cos 2n \vartheta_{nk} \quad (3.16)$$

$$V_n^0 = -2 \int_0^1 \frac{d\eta}{\eta} e^{-a\eta} I_n(a\eta)$$

The size of the region occupied by the nonlinear resonance in J as well as the resonance half-width in the frequency ν can be readily obtained from (3.16):

$$2(\Delta J)_{nk} = 2q_{\max} = 4 \sqrt{\frac{\varepsilon V_n^0}{(\Delta v)_j^2}} \quad (3.17)$$

$$(\Delta v)_{nk} = (\Delta J)_{nk} \cdot (\Delta v)_j^2 = 2 \sqrt{(\Delta v)_j^2 \cdot \varepsilon V_n^0}$$

The approximation in which the Hamiltonian (3.15) has been obtained is known as the approximation of moderate nonlinearity [7,14]. It means physically that if the unperturbed motion is essentially nonlinear and the perturbation is weak, then the size of the resonance region in J will be small compared to the resonance value of the action: $\Delta J \ll J^{(n,k)}$. The second condition of the moderate nonlinearity is that the change ΔJ must be much smaller than the distance between the two neighbouring resonance values of the motion: $\Delta J \ll J^{(n',k')} - J^{(n,k)}$. For the frequency this implies that the width of the nonlinear resonance $2(\Delta v)_{nk}$ must be much smaller than the distance between the two closely spaced resonances:

$$2(\Delta v)_{nk} \ll \nu_{n',k'} - \nu_{nk}; \quad \nu_{nk} = \frac{m_0 k}{2n} \quad (3.18)$$

Actually, (3.18) is the condition for the applicability of the averaging method which allows for the neglecting of all resonances except ones.

The peculiarity of the system under consideration is that the pendulum approximation (3.16,3.17) appears to be more rigid

than the approximation of moderate nonlinearity (3.15). This is associated with the particular type of perturbation for which, in general, it is necessary to take into account the infinite number of harmonics with $l_0 \neq 1$ for the single resonance (n,k) . However, the numerical calculation shows that the contribution of the second term into the sum (3.15) does not exceed 20% even for $n = 3$. When $n > 3$ the terms in the sum (3.15) decrease more rapidly so that the simple estimates (3.17) can be used to obtain the width of the nonlinear resonance.

The latter estimate has been obtained for $a > 25$, which corresponds to the maximum displacement $x_m > 10\sigma$. If a is increased further ($a \gg 1$) the relation $V_{2n}^0(a)/V_n^0(a)$ approaches unity. This indicates that the pendulum approximation is not appropriate at large values of x . However, from a practical point of view the most interesting situation is when the particle displacement x is only several beam widths. The particle diffusion created by the overlap of the nonlinear resonances in this region ($x < 10\sigma$) (see § 4) results in a considerable change for the worse in the real experiments.

Compare now the analytical estimates with the results of computer simulations [30]. The structure of the phase plane (X,P) for the mapping (2.14) with values $m_0 = 2$, $\nu = 3.08$ is illustrated in Fig. 7a. The high-order resonances $k = 3n + 1$, $n = 8, 10, 11, 12$ that grow as they move away from the center are

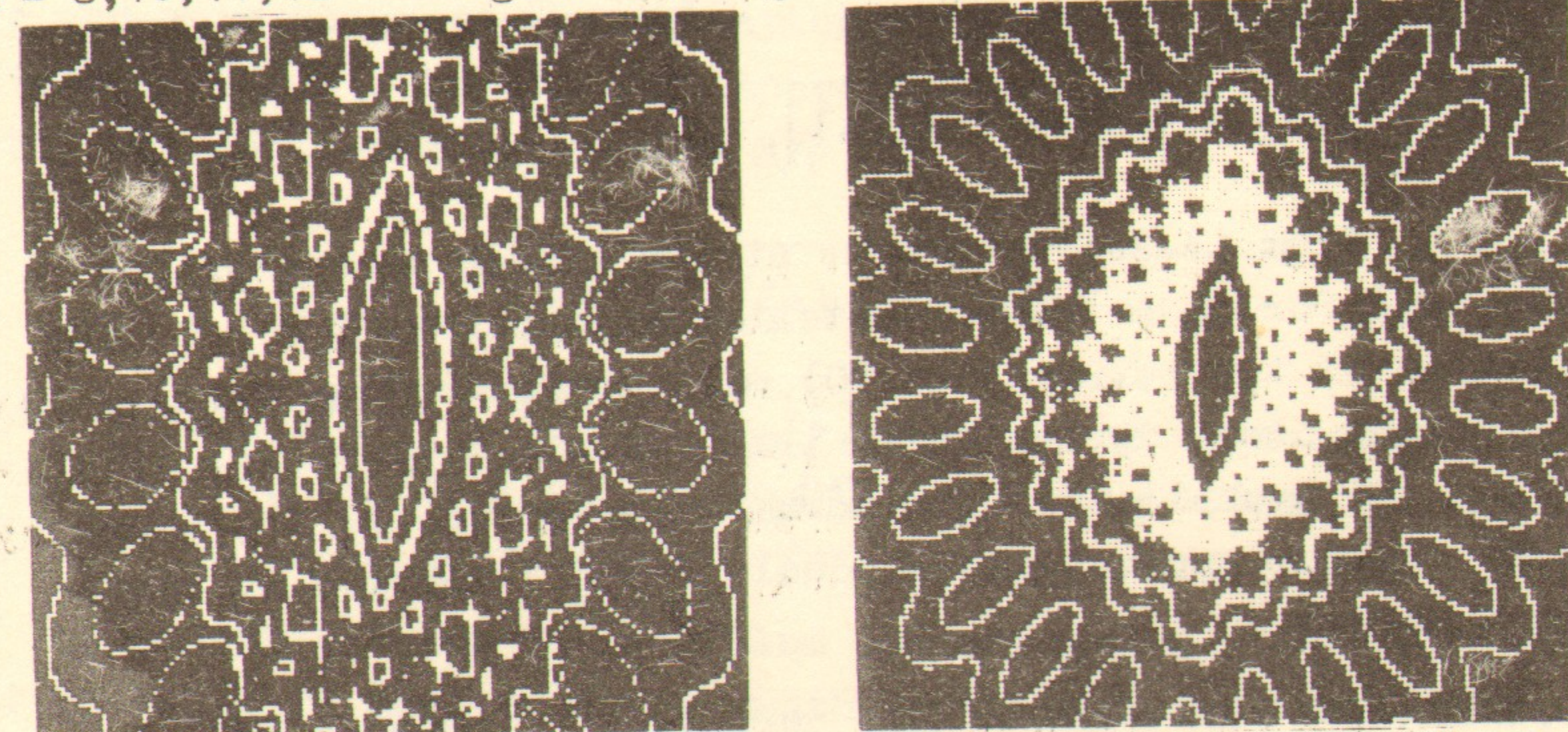


Fig. 7. The phase space for $\nu = 3.08$ Fig. 7a - for $\xi = 0.20$; $|X| \leq 30$; $|P| \leq 15$; Fig. 7b - for $\xi = 0.48$; $|X| \leq 30$; $|P| \leq 30$.

clearly defined in the figure. Since $n \gg 1$ and a is not very large, the location of the resonances can be derived from (3.8, 3.9):

$$\frac{m_0 k}{2n} - \nu = \frac{m_0 \xi}{a} \left\{ 1 - e^{-\bar{a}} I_0(\bar{a}) \right\}; \quad \bar{a} \equiv a_{nk} \quad (3.19)$$

The derived formula (3.19) gives satisfactory accuracy in comparison with the numerical data. For example, for the parameters in Fig. 7a the accuracy of the determination of the position of the resonance center in x grows rapidly as the resonance number is increased and reaches 35%, 15%, 10%, 2% for $n = 8, 10, 11, 12$, respectively. The discrepancy for $n = 8, 10$ might be explained by the influence of the parametric resonance $n = 1$ the detuning from which is not large ($\delta_1 = 0.08$). As we know (§ 2), in the linear approximation this leads to the stretching of the phase ellipse along p by a factor of β/β^* . However, due to the nonlinearity, the stretching must depend upon the transverse energy. This dependence can be taken into account in the following way. When comparing the nonlinear dependence of the tune shift $\Delta\nu(a)$ (3.9) to the linear approximation $\Delta\nu = m_0 \xi$ it is seen that they formally coincide if the strength parameter ξ depends upon a according to (3.9): $\xi \rightarrow \frac{\xi}{a} \{1 - e^{-a} I_0(a)\}$. Hence, if the change Δa is small compared to a , the relation β/β^* (2.19) may be replaced by:

$$\beta/\beta^* = \sqrt{1 - 4\pi^2 \xi^2 g^2(a) + 4\pi \xi g(a) \text{Ctg} \mu} \quad (3.20)$$

$$g(a) = \frac{1}{a} [1 - e^{-a} I_0(a)]$$

For $a \ll 1$ from (3.20) we arrive at the linear approximation (2.19), and for $a \gg 1$ the stretching disappears: $\beta/\beta^* \rightarrow 1$. The comparison of the estimate (3.20) with the numerical results /30/ gives satisfactory agreement in the determination of the relation β/β^* . For example, for the parameters in Fig. 7, the accuracy of β/β^* (which approximately equals P_m/X_m) appears to be no worse than 20%.

Thus, the influence of the parametric resonance can be

taken into account by means of renormalization $\beta \rightarrow \beta^*$ (3.20) and $\xi \rightarrow \xi^*$ in the Hamiltonian (3.4). But from (2.19) we see that $\xi/\xi^* = \beta/\beta^*$. Therefore, $\varepsilon = \varepsilon^*$ and since $a = a^* = (x_m/2\sigma)^2$ such a normalization for the initial data $x_0 = x_m, p_0 = 0$ does not change the value of the nonlinear perturbation at all. On the other hand, the tune shift change (due to $\frac{\partial a^*}{\partial J} = \frac{\beta^*}{2\sigma^2} + \frac{J}{2\sigma^2} \frac{\partial \beta^*}{\partial J}$) and becomes equal to

$$\Delta\nu(a) = m_0 \xi^* g(a) \left\{ 1 - a \frac{\xi^*}{\xi} \cdot \frac{\partial}{\partial a} \left[\frac{\xi}{\xi^*} \right] \right\} \quad (3.21)$$

where $\xi^* = \xi \beta^*/\beta$ and $g(a)$ are determined by (3.20).

The method used here allows us to take into account the main effect of the parametric resonance. Due to this, the nonlinear tune shift (3.21) becomes also dependent on the phase shift μ . The expression (3.21) agrees with the numerical results better than does (3.19) in the region where the effect of the parametric resonance is strong. For example, for the data in Fig. 7 the accuracy of the determination of the resonance location for $n=8$ becomes no worse than 7%, instead of 35%, and for $n = 10, 11, 12$ - better than 5%, 2%, 1%. For large values $a \gg 1$ eq. (3.21) is simplified and if $\pi \xi \ll a \text{Ctg} \mu$ then $\Delta\nu(a) \approx m_0 \xi / \left[a \sqrt{1 + \frac{4\pi \xi}{a} \text{Ctg} \mu} \right]$.

It should be noted that the nonlinear shift dependence $\Delta\nu(a)$ on the energy (3.21) can be improved step by step using more and more accurate approximations for β/β^* . For example, instead of (3.20), in the next approximation we can derive from (3.21) the following dependence β/β^* :

$$(\beta/\beta^*)_1 = \sqrt{1 - 4\pi^2 \xi^2 g_1^2(a) + 4\pi \xi g_1(a) \text{Ctg} \mu} \quad (3.22)$$

where $g_1(a) = g(a) \left\{ 1 - a \frac{\xi^*}{\xi} \cdot \frac{\partial}{\partial a} \left[\frac{\xi}{\xi^*} \right] \right\}$. Another renormalization according to (3.22) for $(\xi/\xi^*)_1$ and $(\beta/\beta^*)_1$ yields instead of (3.21) even more accurate approximation for $\Delta\nu(a)$.

As was mentioned, the pendulum approximation (3.17) can be used to evaluate the resonance width for $n \gg 1$. In particular, from these estimates it follows that the resonance width (in J)

grows proportionally to a , i.e., to the energy, when the resonance moves away from the center. Therefore, if the nonperturbed tune reaches the resonance from below, the resonance area grows rapidly and approaches the infinity (see Figs. 6-8).

§4. The Stochasticity Criterion

Consider now the factors that cause a strong instability of the motion in our model. As we have already mentioned, the single nonlinear resonance stabilizes the motion. This is illustrated in Fig. 6a, where at a given value of ξ the center becomes unstable, but the growth of the resulting oscillations is limited by the nonlinearity. Beyond the resonance regions, the trajectories are also deformed by the perturbation, however, they remain stable too (see also Fig. 7a). The only place where the instability arises is in a small region near the separatrix of every resonance. As was shown by analytical and numerical studies [40,14,7], under the influence of any small perturbation there arises the so-called stochastic layer near the separatrix. The motion in this layer appears to be always unstable. This is caused by the fact that the frequency of nonlinear oscillations near the separatrix is very small. Therefore, any perturbation caused by nonresonance terms may have a strong effect. This produces a local instability in which two initially neighbouring trajectories diverge rapidly, becoming far apart in only a few oscillation periods. Nevertheless, such an instability in the case of one-degree of freedom does not create any notable diffusion of the phase trajectory since at small perturbations the width of the stochastic layer is exponentially small and the layers are separated by stable trajectories (see Figs. 6a-7a). This phenomenon is consistent with a strict numerical theory, namely, that of Kolmogorov-Arnold-Moser (KAM) [41-43]. According to this theory, in the nonlinear system the action of a sufficiently small perturbation destroys only a part of the so-called resonance tori, those that satisfy certain resonance relations. The remaining tori are only slightly deformed and the motion along

their surface remains stable (for more details see, e.g., Ref. [44]). In our case, the destroyed tori are the separatrices of nonlinear resonances (see Figs. 6a-7a).

However, the KAM theory does not provide the answer to a rather important practical question, namely, at what critical perturbation does the destroying of tori create a strong instability. The latter term refers to an instability strong enough to create a diffusion over a sufficiently large area of the phase space. Defined in this way the instability is very weak inside the stochastic layer. Naturally, the search for the critical perturbation strength in particular physical systems is an extremely important problem. However, this problem cannot be solved in terms of any strict theory. In this case, the semi-qualitative approach suggested by B.V.Chirikov [12,14,7], seems to be very useful. The physical idea of this approach will be illustrated with our model.

The analysis (§3) shows that as the perturbation increases, the regions occupied by nonlinear resonances tend to grow and eventually overlap at a certain critical perturbation strength.

The trajectory will thus be capable of passing from one resonance into another. This situation is illustrated in Fig. 7b, where the perturbation strength ξ is well above that in Fig. 7a. It is seen that such an increase of ξ produces a large area which is occupied by only one trajectory. The motion in this area appears to be chaotic or, as they say, stochastic. Thorough numerical studies (see, e.g., Refs. [6-7]) have shown that the motion really does possess statistical properties.

The appearance of stochastic motion in a dynamical system, in which no extrinsic irregularity exists, can be attributed to the local instability of the motion. In this case two neighbouring trajectories diverge rapidly from each other. If we denote the distance between two nearby trajectories in the phase space by $\bar{\Delta}$ on the average, its growth will follow the law $\bar{\Delta} = \bar{\Delta}_0 e^{ht}$. The value h is called KS-entropy (see, e.g., Ref. [11]) and

determines the average rate at which trajectories diverge in the phase space. In the nonlinear oscillation system, strong local instability always arises as soon as the regions of nonlinear resonances overlap [7]. It is for this reason that B.V.Chirikov has suggested that the condition of overlapping nonlinear resonances be a criterion for stochasticity.

For the model under consideration, the stochasticity leads to a rapid increase in the particle's transverse energy, which is an extremely undesirable effect in real facilities. Therefore, it seems very important to determine the parameter values at which the motion will be the most stable. Fig. 8a illustrates the situation when a stable area in the phase space near $X=P=0$ is rather large. This may be accounted for by the fact that slightly above the parametric resonance the harmonics of the nonlinear resonances are large: $n \gg 1$. These resonances are therefore small and become of appreciable size only for $a \gg 1$. For $\nu = 3.2001$ at the same perturbation $\xi = 0.24$ (Fig. 8b) the main stochasticity area shifts towards smaller values of X and is reduced in size. In this case, only two resonances actually overlap: $n=4$ and $n=3$. In contrast to Fig. 8a, for large values of X the motion is stable. This is due to the fact that the value of X is slightly larger than the resonance value $\nu_n = 1/5$. Hence, for $X \gg 1$ strong resonances are absent. But if we take $\nu \approx 0.32$ which is slightly below the resonance value $\nu_n = 1/3$ (Fig. 8c), the area occupied by the resonance $n=3$ appears to be very large (see § 3).

Fig. 8 illustrates the situation when the perturbation strength is slightly above the critical value. Here the resonances either touch each other or partially overlap. Nevertheless, this is sufficient for a strong diffusion to arise along the destroyed separatrix of different resonances. Correspondingly, the Chirikov criterion for stochasticity can be then written:

$$s \equiv \frac{2(\Delta\nu)_n}{\nu_{n+1} - \nu_n} \geq 1 \quad (4.1)$$

where $2(\Delta\nu)_n$ is the maximum width of the nonlinear resonance in

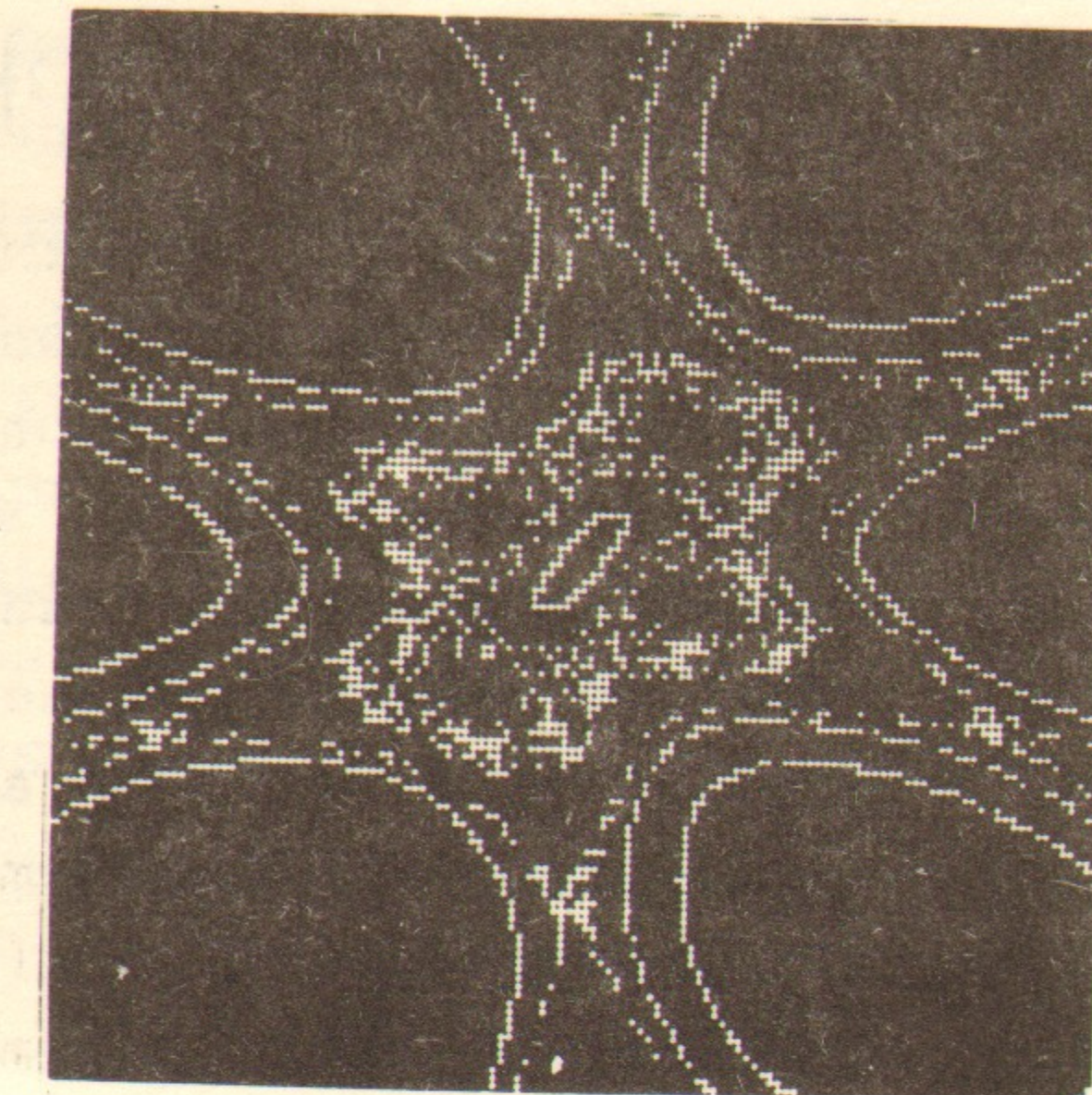
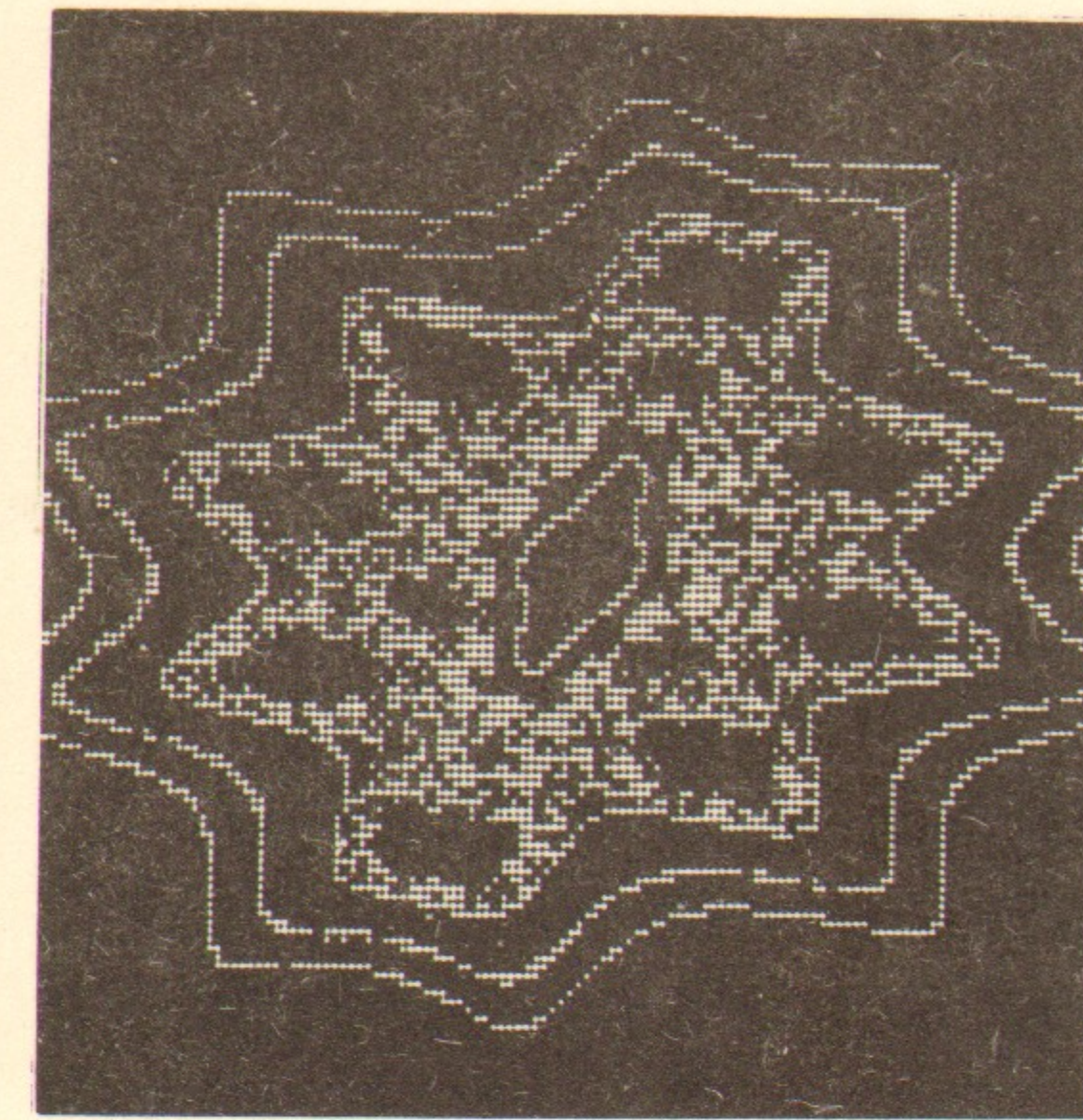
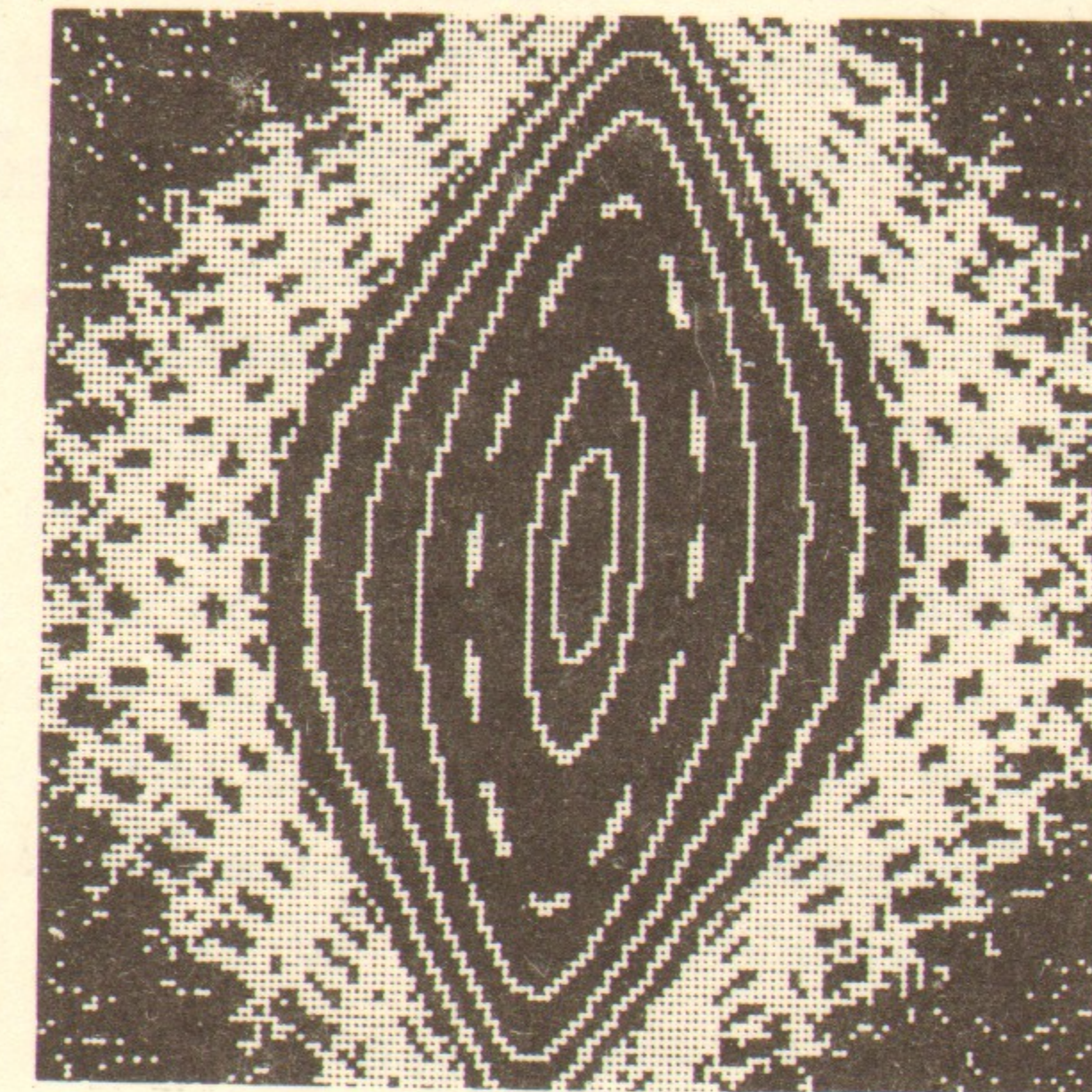


Fig. 8. The phase space for different values of the tune ν slightly above the stochastic threshold. Fig. 8a - for $\nu=3.04$; $\xi=0.32$; Fig. 8b - for $\nu=3.2001$; $\xi=0.24$ Fig. 8c - for $\nu=3.32$; $\xi=0.24$ In all figures $|X| \leq 10$; $|P| \leq 15$.

frequency, and $\nu_{n+1} - \nu_n$ is the distance between the neighbouring resonances.

For given values of ν (see Fig. 8) the distance between the main neighbouring resonances is $\nu_n - \nu_{n+1} = \frac{1}{n} - \frac{1}{n+1} = \frac{1}{n(n+1)}$. Since $n \geq 3$ the pendulum approximation (3.16-3.17) can be used. We then obtain:

$$S = 4m_0 \xi n(n+1) \sqrt{2f_n(a_n)g'(a_n)} \quad (4.2)$$

$$f_n(a) = \int_0^1 \frac{e^{-a\eta}}{\eta} I_n(a\eta) d\eta; \quad g'(a_n) = \left. \frac{\partial g(a)}{\partial a} \right|_{a=a_n}$$

where $g(a)$ is determined by the nonlinear betatron tune shift (3.9):

$$g(a) = \frac{1}{a} \left\{ 1 - e^{-a} I_0(a) \right\}$$

The condition for the touching of separatrices: $S = 1$ may be taken, in a first approximation, as a condition for the appearance of strong diffusion. Thus, the critical value of the parameter ξ_c depends upon m_0, ν, n, a_n . It should be noted that for a given value of the betatron tune ν , the resonance number n and the resonance value a_n are dependent. The obtained expression (4.2) reflects a fairly complicated dependence of the criterion (4.1) on the model parameters. In particular, for the perturbation εV_n^0 (which is proportional to $f_n(a_n)$) one fails to obtain a simple estimate since the integral in (4.2) depends mainly upon the ratio a to n . In the limiting cases, for $a/n \gg 1$ or for $a/n \ll 1$ an estimate of the integral can be easily found. It often appears, however, that the most interesting cases from a practical point of view correspond to intermediate values of a/n . For $\nu = 3.2001$ the condition (4.2) gives a critical perturbation value of $\xi_c = 0.32$. The numerical value for ξ_c reported in Ref. /30/ is in satisfactory agreement with the analytical estimate. For comparison,

Fig. 9 gives the results of numerical experiments on the determination of ξ_c for system (2.14). This is the condition for the touching of separatrices of the main resonances in the region of restricted $X_{\max} = 10$. A strong instability created by the overlap of these resonances is well illustrated in Fig. 8a, b, c.

It should be noted that the meaning of the critical perturbation itself is somewhat conventional. For example, we may be interested in the creation of a not so large stochastic region for certain values of X_m say, for $X_m = 1-2$. In this case, we should consider the overlap of only those nonlinear resonances that are located in this region. We should also take into account the resonances of higher harmonics as well as additional resonances caused by various modulations (see § 5).

When analyzing the dependence ξ_c (curve II, Fig. 9), we see, first of all, that ξ_c is only slightly dependent on $\{\mu/\pi\} = \{\nu\}$ over fairly broad ranges. However, the value ξ_c in /30/ was determined as a condition for the appearance of a large stochasticity area caused by the overlap of main resonances for $X_m < 10$. Therefore, the size of the stochastic area and its location vary depending upon ν . This is especially clear when approaching the parametric resonance from above. In this case, when $\{\nu\} \ll 1$ the motion becomes much more stable (see Fig. 8). A sharp increase in ξ_c (Fig. 9) is due to the parametric resonance which reduces the tune shift $\Delta\nu$ (see § 2 and § 3). Furthermore, in this region of variations ν there exist only resonances of large harmonics $n \gg 1$.

The strong effect of the parametric resonance $n = 1$ on the total motion is, evidently, the most characteristic feature of nearly linear mappings. At small displacements, when $X_m \ll 1$, the action of the parametric resonance can be linearly approximated (§ 2) and can lead to the stretching of the phase ellipse such that ultimately the center $X=P=0$ appears to be destroyed. For $X_m \gg 1$ the parametric resonance becomes essentially nonlinear and occupies a large area in the phase space even if the detuning from the resonance value $\delta_1 = \nu - m_0 k/2$ is large

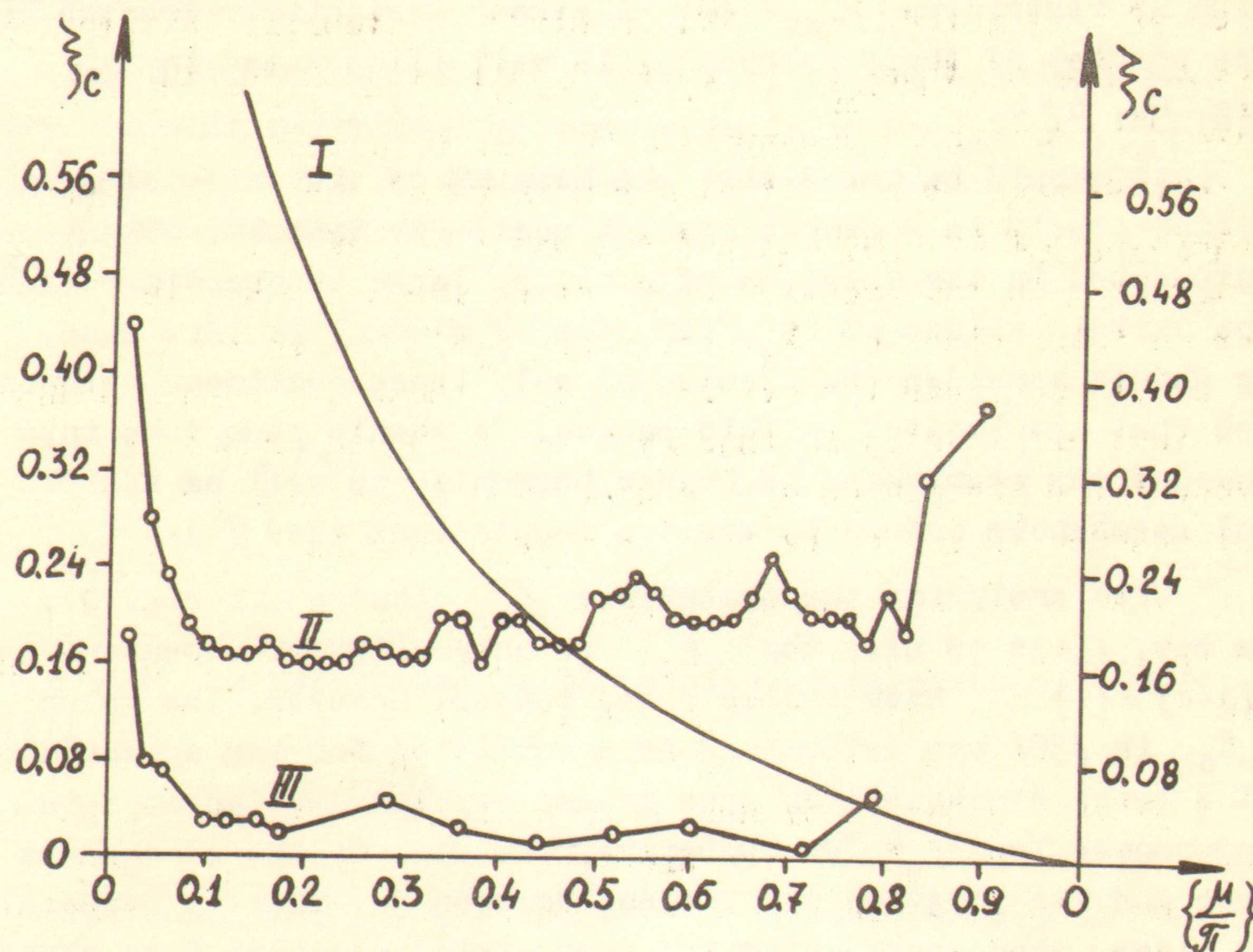


Fig. 9. The data of the computer simulation from Ref. /30/ for basic mapping (2.14). The curve I is the linear stability condition (2.15). The curve II—the critical value of the strength parameter ξ_c for which the separatrices of the main resonances touch each other (see Fig. 8). Curve III represents ξ_c for the case of modulation (5.1) with the data: $A_s = 1.5$; $\nu_s = 0.01$. (see § 5 and Fig. 10). The horizontal line corresponds to the fractional part of μ/π .

(Fig. 6). Note also that an exact condition of the resonance $\nu = m_0 k/2$ for even values of $m_0 k$ coincides with the external linear resonance condition $\Omega_0 = n_0$ where Ω_0 is the frequency of the external perturbation and n_0 is an integer. Although in our model such resonances are absent because the force is only dependent upon the coordinate, in general, they can exist. Therefore, it seems interesting to investigate the combined action of the parametric and external resonances.

According to the analysis, taking into account the parametric resonance can substantially change the estimate of the overlap criterion (4.2). It is necessary, therefore, to renormalize β and ξ in the same manner as it was done in § 3 (see (3.20)). This implies that in (4.2) the parameter ξ must be replaced by ξ^* and the dependence $g(a)$ — by the dependence determined in (4.2). As a result, the estimates (4.2) become even more complicated.

The derived condition (4.1-4.2) is approximate even far from the parametric resonance. It may be somewhat improved, for example, by taking into account the difference in the size of neighbouring resonances n and $n+1$. It seems natural then to replace the value $(\Delta\nu)_n$ by $\frac{1}{2}[(\Delta\nu)_{n+1} + (\Delta\nu)_n]$ in (4.1).

It should be noted, however, that inspite of this improvement, the stochasticity criterion (4.1-4.2) is, in principle, still an approximate condition. This is related to the fact that the expression for the nonlinear resonance width has been obtained by neglecting the action of neighbouring resonances. But this approximation is not valid close to the resonance touching. It is clear that the resonances begin to interact with each other even before the touching. Therefore, the stochasticity condition may be improved by taking into account the high-order resonances which lie between the main resonances. As was reported in Ref. /7/ for mapping (1.1) taking into account the high-order resonances and the finite width of the stochastic layer around the separatrix reduces the critical value of the parameter k_0 by approximately a factor of 2.5. The comparison

has shown good agreement ($\approx 10\%$) between the improved analytical estimates and the numerical results. Another interesting approach to finding the critical perturbation has been suggested in Ref. /45/. As a condition for the appearance of the infinite diffusion (in momentum p) in (1.1) /45/ the condition of a full destruction of very high-order resonances which lie between the low-order resonances was used.

Compare now the analytical estimates obtained for our model with the computer results. Consider, for example, the situation when the overlap of two main resonances ($n=3$ and $n=4$) creates a large stochastic area (Fig. 8b). The numerical value of the strength parameter ξ_c for which the resonances touch each other has been reported in Ref. /30/. According to the data in Fig. 9, $\xi_c \approx 0.16$. Since the unperturbed betatron frequency ν is $\nu = 3.2001$ and is well above the parametric resonance ($\delta_1 = \nu - 3 = 0.2001$), we use the simplified estimates (4.2) without taking into account the parametric resonance. As is seen in Fig. 8b, the size of resonances $n=3$ and $n=4$ differs significantly. Further we take this fact into account for deriving the stochasticity limit. As a result, we obtain $\xi_c^{th} \approx 0.22$, which exceeds the numerical value by only a factor of 1.37. Therefore, even simplified estimates give us the correct result for the critical value of ξ_c . The further improvement of the analytical estimate for ξ_c is related, first of all, to taking into account the high-order resonances and the finite width of the stochastic layer around the separatrix.

§ 5. Time-Dependent Mappings

After comparing the results of numerical simulation /30/ with those of real experiments on colliding electron-electron and electron-positron beams /46-48/, the model described by mapping (2.11) does not seem satisfactory. The values for ξ_c obtained by numerical simulation (fig. 9) are found to be significantly higher than the corresponding experimental values ($\xi_c \approx 0.05-0.08$). One of the important factors that can decrea-

se ξ_c (in the 2-dimensional model) is the modulation of certain model parameters*. Leaving aside the physical meaning of this phenomenon which is related to some peculiarities of the particles' motion in the accelerator /49-52/, consider now the most important types of modulation.

If in the reference system of a particle the center of the strong beam slowly oscillates, the strength of the particle-beam interaction will also oscillate. For our model this can be taken into account by proceeding from x to a new variable

$$u_s : \quad u_s = x + A_s \cos \nu_s t \quad (5.1)$$

in the force (2.13). Here A_s and ν_s characterize the modulation amplitude and frequency ($\nu_s \ll \nu$), respectively. Then the mapping (2.14) becomes dependent on a dimensionless time given by the number of kicks.

A numerical study of the mapping (2.11) involving (5.1) has shown /30/ that the critical value ξ_c decreases considerably with modulation. This is illustrated by curve III in Fig. 9 for which $A_s = 1.5$ and $\nu_s = 0.01$. A typical phase plane is shown in Fig. 10. With the time-dependent mapping the determination of ξ_c becomes more complicated. This results from the oscillation of the location of the nonlinear resonance. In this situation, the overlap of the main resonances and the trajectory movement from one resonance to another can be easily observed on a display which is connected on-line with the computer /30/. The trajectories for different initial data are clearly seen in Fig. 10. As is seen in Fig. 10b, when $\xi = 0.04$, the resonance $n=7$ already overlaps its inside neighbouring resonance.

Another way to represent the system motion in the case of modulation is to plot the trajectory on the phase plane not at each step of the mapping, but at the modulation period T_s ,

* The role of increasing the degrees of freedom will be discussed in §6.

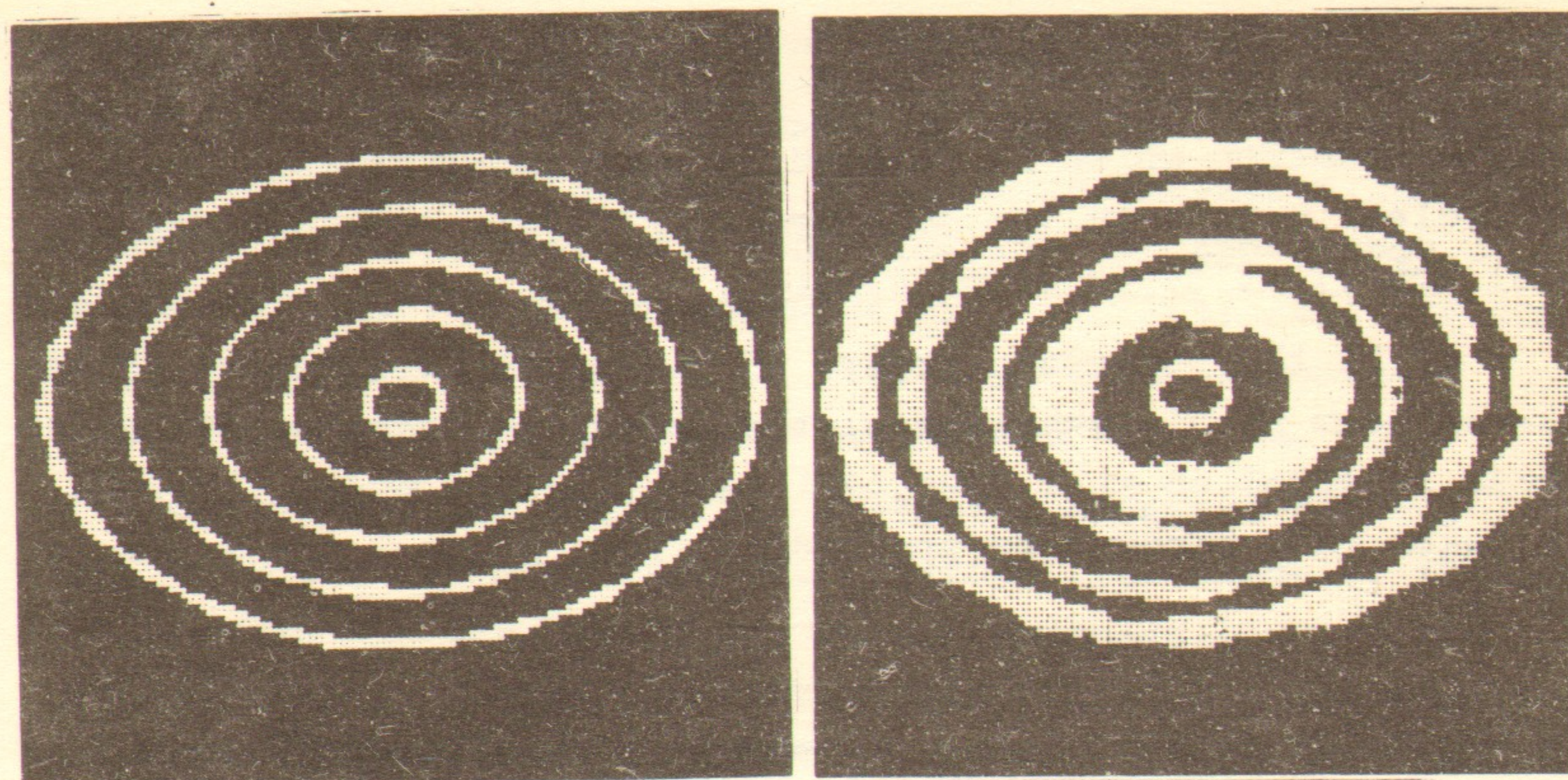


Fig. 10. The phase space for the mapping (2.14) with the modulation (5.1) and the data: $\nu = 3.12$; $\nu_s = 0.01$; $A_s = 1.5$; $|X| \leq 10$; $|P| \leq 15$. Fig. 10a - The stable trajectory below the stochasticity threshold for $\xi = 0.02$. Fig. 10b - The overlap of the two resonances for $\xi = 0.04$.

/33/. Then all additional resonances will be clearly seen on the phase plane. This is due to the fact that in a modulation period the total mapping will not depend on time. The total mapping equals the product of T_s nonlinear mappings (2.14). Although such an expression is impossible to obtain, for the computer experiments this method of representation appears to be very convenient (see Ref. /33/).

The strong effect of modulation in our system results from the appearance of many additional side-band resonances. The Hamiltonian corresponding to mapping (2.11) is in J and Ψ variables (see §2):

$$H = J\nu + \varepsilon \int_0^1 \frac{1 - e^{-u_s \eta}}{\eta} d\eta \cdot \sum_{k=-\infty}^{+\infty} e^{ik\theta} \quad (5.2)$$

$$u_s = \frac{(x + A \cos \nu t)^2}{2\sigma^2};$$

$$x = \sqrt{2J\beta} \cos \Psi$$

Near a single resonance (§3) the Hamiltonian has the form

$$H = J\nu + \varepsilon \int_0^1 \frac{d\eta}{\eta} \left\{ 1 - e^{-(a+d)\eta} I_0(a\eta) I_0^2(r\eta) I_0(d\eta) \right\} - \quad (5.3)$$

$$- 2\varepsilon \int_0^1 \frac{d\eta}{\eta} e^{-(a+d)\eta} \sum_{p,q,m,k,n=-\infty}^{+\infty} I_n(a\eta) I_p(r\eta) I_q(r\eta) I_m(d\eta) \cos \vartheta_{npqkm}$$

where the dependence on the unperturbed phase Ψ is given by:

$$\vartheta_{npqkm} = (2n+p+q)\Psi + (p-q+2m)\varphi - k\theta \quad (5.4)$$

$$\dot{\Psi} = \nu + \Delta\nu; \quad \dot{\varphi} = \nu_s; \quad \dot{\theta} = m_0$$

and the introduced values a, r, d are expressed through x_m and A_s via the formulas

$$a = \left(\frac{x_m}{2\sigma} \right)^2; \quad d = \left(\frac{A_s}{2\sigma} \right)^2; \quad r = \sqrt{ad} = \frac{A_s x_m}{2\sigma^2} \quad (5.5)$$

From (5.4) we obtain the resonance condition

$$\nu + \Delta\nu = \frac{m_0 k + (p-q+2m)\nu_s}{2n+p+q} \quad (5.6)$$

The spectrum of resonance frequencies (5.6) involving modulation is much more complicated than (3.5). An analysis of (5.6) suggests that even for $\nu_s = 0$ ($A_s \neq 0$) there exist additional resonances not present in (3.5). Note that these additional resonances can be induced by time-independent shift of the beam center even without the modulation. The condition $p+q = \pm 1$ corresponds to the first side-band resonance. The distance between this resonance and the main resonance n is $(\Delta\nu)_s = \frac{km_0}{2n(n+1)}$ which for $n \gg 1$ is half the distance between the main resonances: $\nu_n - \nu_{n+1} \approx km_0 / (2n^2)$. As follows from (5.3), the amplitudes of the additional resonances are determined mainly by the condition $p=0, q=1$ and $p=1, q=0$ and depend upon r . For $r > 1$ additional and main resonances become comparable and the critical value ξ_c must decrease by a fac-

tor of 2. Since the denominator in (5.6) can be odd, for $A_s = 0$ the degeneration observed for (2.14) is absent. This is due to the fact that the interaction potential $V(x)$ is not symmetric with respect to the sign of the coordinate x . For $v_s \neq 0$ the distance to the nearest side band resonance is $(\Delta v)_{ns} \approx v_s/n \ll v$. The strength of the side band resonances falls as the values of p, q and m are increased (see (5.3)). However, the distance between the side-band resonances is very small, and they will overlap at much smaller values of ξ than the main resonances. Then the overlap of these small resonances results in a weak diffusion*. If the total region of overlap of side-band resonances (in frequency v) is comparable to the distance between the main resonances, this leads again to the overlap of the main resonances and to a strong diffusion, as in the case of the time-independent mapping.

It is, in this case, difficult to derive analytical estimates for the condition of strong stochasticity as is apparent from the form of Hamiltonian (5.3). However, even in this case, some conclusions can be drawn, especially when comparing different types of modulation. Consider, for example, the situation in which the period L of the beam-particle interaction is slowly oscillating. For (2.11) and (2.14) this leads to modulation of the phase advance between the interaction points:

$$\mu = \mu_0 + B_0 \cos v_s t \quad (5.7)$$

In the single resonance approximation the Hamiltonian for such a modulation is

$$H = Jv + \varepsilon \int_0^1 \frac{d\eta}{\eta} \left\{ 1 - e^{-a\eta} I_0(a\eta) \right\} - 2\varepsilon \int_0^1 \frac{d\eta}{\eta} e^{-a\eta} I_n(a\eta) \cdot J_m(b_n) \cos(2n\psi - k\theta + m\phi) \quad (5.8)$$

* Here "weak diffusion" means that the diffusion is restricted to a small area of the phase space due to the overlap of only a few side-band resonances.

Here $J_m(b_m)$ is the usual Bessel function of m -th order with the argument $b_n = B_0 m_0 n / v_s$. The resonance condition for (5.8) can then be written

$$v + \Delta v = \frac{km_0 + mv_s}{2n} \quad (5.9)$$

A comparison of (5.9) with (5.6) tells us that the spectrum of resonance frequencies is simpler for this type of modulation than for modulation (5.1). Specifically, for (5.8) the degeneration is not removed and the resonance harmonics are only even. However, the distance between the additional resonances $(\Delta v)_{ns} = v_s/2n$ is two times smaller than for (5.1). The most essential difference between the modulation under consideration and the previous one is as follows. The strength of each side-band resonance $m \neq 0$ for any n depends upon $J_m(b_n)$ and for $b_n \gg 1$ changes slightly with increasing m . For the previous case (5.3), the contrary is true and the strength of the side-band resonances falls sharply as m is increased (for $d \ll 1$). The estimate for the total width of all the side band resonances can be derived directly from (5.8). The maximum value of m^* can be found from condition $J_{m^*}(b_n) = \text{const}$: $m^* < b_n = B_0 m_0 n / v_s$. For $B_0 / v_s \gg 1$ we obtain a fairly wide range of frequencies. If the total width of these resonances is comparable to the distance between the main resonances, the overlap of side-band resonances creates a strong diffusion along the main resonances. This is the case for $B_0 > B^c \approx \frac{1}{m_0 [v]}$, where $[v]$ is the integer part of the frequency v . As is seen, the estimate B^c does not involve the modulation frequency v_s , since with the decreasing of v_s the value m^* increases while the total frequency range occupied by side-band resonances remains constant.

It should be noted that even the overlap of several side band resonances may turn out to be essential for practical applications. For example, in a somewhat different model /33/, the overlap of 3-4 resonances created a stochastic region of about $\Delta X_m \approx 1.5$ in width. This means that the density of charged

particles in the beam cross section will decrease. As a result, the interaction between such beams will be also lowered. Therefore, in storing rings the influence of side-band resonances may appear to be rather significant /33,49-52/.

Another modulation type, which is less efficient at first glance than the above modulation, seems to be worth noting as well. Assume, for example, that due to some physical effects (see, e.g., /33/), the perturbation parameter ξ cannot be constant at the interaction points and its dependence on the dimensionless time t is determined by a weak modulation :

$$\varepsilon = \varepsilon_0 + d_s \cos v_s t \quad d_s \ll \varepsilon_0 \quad (5.10)$$

In the perturbation spectrum there are only two side band resonances, one on each side of the main resonance : $v_n \pm v_s/(2n)$. However, taking into account effects of second order in d_s/ε_0 we have again the above discussed modulation of the parameter (5.7). In fact, the first order approximation gives only a weak modulation of the unperturbed phase. In the second order approximation this modulation also influences the perturbation and therefore there appears a wide spectrum of additional resonances. This situation was investigated in detail in Ref./33/.

§6. Conclusion remarks

The applicability of mappings and, in particular, of the nearly linear mappings, is much wider than it might seem at the first glance. In our example, the differential equation (2.1) can be easily reduced to a mapping because the perturbation is a delta function. Therefore, we can easily integrate the unperturbed motion in the time interval between the kicks and then take into account the influence of the kick. In general, for a time-dependent perturbation the differential equation can be reduced to a mapping by integrating the equation of motion over a finite time interval. This integration may be quite complicated. In some cases, however,

this approach is much simpler than a complete numerical solution of the problem. In fact, it may not even be necessary to find an exact mapping. An approximate one may be sufficient for certain applications /53-54, 4-5/.

The mapping is often constructed using the so-called Poincare' method (see, e.g., Ref./2/). In this case the mapping describes exactly but not completely the motion of a continuous dynamic system. In a sense, a two dimensional mapping is equivalent to a continuous dynamical system with a three-dimensional phase space. In particular, it is the case of a conservative system with two degrees of freedom. Clearly, the analytical and numerical investigations of mappings are much simpler than the integration of differential equations.

The model considered above clearly illustrates the main properties of nearly linear mappings. First of all note the strong influence of the parametric resonance on the motion of the system for a wide range of the model parameters. As compared to other nonlinear resonances, the parametric one has rather special features. At small amplitudes it produces a linear effect, the rapid growth of transverse oscillations at the interaction points. At large amplitudes, above the linear stability limit it leads to nonlinear stabilization of the particle motion. Consequently, it is often necessary to take into account the influence of the parametric resonance in the derivation of various analytical estimates.

Another feature of nearly linear systems is that the pendulum approximation, in general, is not valid. This is seen, in particular, when the low-order resonances including the parametric resonance, are considered. Nevertheless, for high-order resonances in the model under study, it appears possible to use the approximation of moderate nonlinearity. The reason for this is a drastic decrease in the resonance strength with an increase of the resonance order. Moreover, there exists a parameter range where the pendulum approximation is quite applicable. From this point of view, a very important problem is the question of how validity of a certain

approximation depends on the type of nonlinear perturbation.

The pendulum approximation is convenient since it provides a universal description of any arbitrary nonlinear resonance and allows for derivation of fairly simple estimates for the resonance overlap criterion. As is shown, for nearly linear systems such a universal method does not seem to exist. Development of a common approach that can combine these both cases, is one of the important problems in the theory of stochastic oscillations.

Concerning the interpretation of our model from the physical point of view and the comparing of the results of computer simulation with real data, it should be mentioned that the twodimensional mapping describes the motion only along one transverse coordinate. In this connection, of special importance is the mutual influence of the motions along the two transverse coordinates. The mapping, which describes a model with two degrees of freedom, becomes four-dimensional and thus complicates both the analytical and numerical investigations. For the system with two degrees of freedom, the number of possible resonances increases drastically. This is due not only to the additional resonances introduced by the motion in Z , but also to the appearance of the new coupling resonances /37, 22-23/. These latter are derived from the total resonance relation $2n_x \nu_x + 2n_z \nu_z - m_0 k = 0$ for $k=0$ (n_x, n_z, k are integers, positive and negative). Consequently, for the stochasticity criterion it is necessary to take into account the possibility of overlapping nonlinear coupling resonances with each other and with one-dimensional resonances.

The four-dimensional mapping has long been a matter of interest (see, e.g., Refs./55-59/). The main difficulty in the numerical study has been the determination of the type of motion. Since the phase trajectory occupies a four-dimensional volume, one has to consider only its projection on a certain cross-section. It becomes difficult to distinguish between the stochastic and regular motion because the areas of nonlinear resonances in such representation cannot be seen. Therefore,

it is common to use some qualitative characteristics, such as the KS-entropy (see §4) which characterizes the mixing rate of the phase trajectories.

Note also that multi-dimensional nearly linear mappings can have specific features not present in two-dimensional ones. This is shown, for example, by some numerical experiments with a conservative system consisting of three linear oscillators with a nonlinear coupling /60/. The frequencies of the unperturbed motion in this system $\omega_1, \omega_2, \omega_3$ are related to each other by two resonance relations: $2\omega_1 = \omega_2$ and $3\omega_2 = \omega_3$. As shown by a study of this motion /60/, the stochasticity criterion does not depend upon the perturbation strength. The perturbation parameter is found to determine only the rate of the stochastic diffusion and not the size of the stochasticity region.

Finally, the author wishes to thank Dr.B.V.Chirikov for fruitful discussions and for critical reading of this work. The author is also grateful to J.L.Tennyson and I.B.Vasserman for many productive conversations and helpful comments as well as to L.F.Khailo for her assistance in computation.

R e f e r e n c e s

1. Transformations Ponctuelles et leurs Applications (Toulouse, 10-14 Sept. 1973), Colloques Internationaux du C.N.R.S. No 229, CNRS, Paris (1976).
2. Yu.I.Neimark, The Method of Point Mappings in the Theory of Nonlinear Oscillations (Nauka, Moskva, 1972) (in Russian)
3. C.Froeschlé, Astron. and Astrophys., 9 (1970) 15.
4. V.N.Melekhin, Zh. Exper. Teor.Fiz. 61 (1971) 1319 ; 68 (1975) 1601.
5. M.A.Liberman and A.J.Lichtenberg, Phys.Rev. A5 : 4(1972) 1852.
6. B.V.Chirikov and F.M.Izrailev, Colloques Internationaux du C.N.R.S. No 229 (Transformations Ponctuelles et leurs Applications, Toulouse, 10-14 Sept. 1973) CNRS, Paris (1976) 409.
7. B.V.Chirikov, Physics Reports, 52 (1979) 263.
8. B.V.Chirikov, Fizika Plasmy 4:3 (1978) 521 ; Preprint 78-67 (Institute of Nuclear Physics, Novosibirsk, 1978).
9. G.R.Smith and A.N.Kaufman, Phys.Rev.Lett. 34 (1975) 1613.
10. G.V.Gadiyak and F.M.Izrailev, Dokl.Akad.Nauk SSSR 218 (1974) 1302.
11. G.M.Zaslavsky and B.V.Chirikov, Soviet Physics Uspekhi 14 (1972) 549.
12. B.V.Chirikov, Atomnaya Energiya 6 (1959) 630.
13. F.M.Izrailev and B.V.Chirikov, Dokl.Akad.Nauk SSSR 166 (1966) 57.
14. B.V.Chirikov, Research Concerning the Theory of Nonlinear Resonance and Stochasticity, Preprint 267 (Institute of Nuclear Physics, Novosibirsk, 1969) (Engl.Trans., CERN Trans. 71-40, 1971).
15. A.J.Lichtenberg and E.F.Jaeger, Physics of Fluids 13, No 2 (1970) 392 ; E.F.Jaeger and A.J.Lichtenberg, Ann.Phys. 71 (1972) 319.
16. J.Ford, The Statistical Mechanics of Classical Analytic Dynamics in "Fundamental Problems in Statistical Mechanics" Vol. 3, ed.E.D.G. Cohen (North-Holland Publishing Company, Amsterdam, 1975).
17. N.N.Bogoliubov and Yu.A.Mitropolsky, Asymptotic Methods in the Theory of Nonlinear Oscillations (Hindustan Publ.Corp., Dehli, 1961).
18. M.Sands, The Physics of Electron Storage Rings, Report SLAC-121 (1970).
19. A.W.Chao, A Summary of Some Beam-Beam Models, Proc. of Symposium on Nonlinear Dynamics and Beam-Beam Interaction, Brookharen Nat.Lab., March 19-21 (1979) 42.
20. E.Coddington and N.Levinson, Theory of Ordinary Differential Equations, (Gordon and Breach, New York, 1965).
21. E.D.Courant and H.S.Snyder, Ann. of Phys., 3 (1958) 1.
22. A.A.Kolomensky and A.N.Lebedev, Theory of Cyclic Accelerators (Wiley, New York, 1966).
23. H.Bruck, Accelaratuers Circulaire de Particules (press Universitaires de France, Paris, 1966).
24. E.D.Courant, IEEE Trans. Nucl. Sci. NS-12 (1965) 550.
25. E.A.Crosbie, T.K.Khoe and R.J.Lari, IEEE Trans. NS-18 (1971), 1071.
26. G.Gumowski and C.Mira, "Proc. 8-th Int.Conf. on High Energy Acc.", CERN (1971) 374.
27. E.Keil, CERN/ISR-TH/72-7 ; CERN/ISR-TH/72-25.
28. A.G.Ruggiero and L.Smith, Stanford (SLAC), PEP-52 (1973).
29. A.Renieri, "Proc.IXth Int.Conf. on High Energy Acc.", Stanford (1974) 414.
30. F.M.Izrailev, S.I.Mishnev and G.M.Tumaikin, Preprint 77-43 (Institute of Nuclear Physics, Novosibirsk, 1977) ;

- F.M.Izrailev, S.I.Mishnev and G.M.Tumaikin, "Proc. Xth Int. Conf. on High Energy Acc.", Serpukhov (1977), v.II, p.302.
31. R.H.G.Helleman, "Statistical Mechanics and Statistical Methods", Ed. U.Landman, p.343-370, Plenum Publ., Co., N.Y. (1977).
 32. R.H.G.Helleman, Exact Results for some Linear and Nonlinear Beam-Beam Effects. To appear in Proc. of (December 17-21, 1979) "Symposium on Nonlinear Dynamic and the Beam-Beam Interaction" ed. M.Month.
 33. J.L.Tennyson "The Instability Threshold for Bunched Beams in ISABELLE", AIP Conf., Proc. of "Symposium on Nonlinear Dynamics and Beam-Beam Interaction", Brookhaven Nat. Lab., March, 19-21, (1979) 158.
 34. S.K.Godunov and V.S.Rjabenjkij, The Difference Schemes (Nauka, Moskva, 1973) (in Russian).
 35. C.R.Eminizer, P.A.Vuillermot, T.C.Bountis and R.H.G. Helleman in "Review of the Beam-Beam Phenomena", BNL-25703 Accelerator Department, Brookhaven Nat.Lab., Upton, N.Y. (1979).
 36. H.Goldstein, Classical Mechanics (Addison-Wesley Press. Inc., Cambridge, 1950).
 37. A.Schoch, CERN Report 57-21 (1958).
 38. G.Guignard, CERN/76-06, Geneva (1976) ; CERN/78-11, Geneva (1978).
 39. A.G.Ruggiero, "Proc. IXth Int.Conf. on High Energy Acc.", Stanford (1974) 419.
 40. V.K.Melnikov, Dokl.Akad.Nauk SSSR 144(1962) 747 ; 148 (1963) 1257 ; Trudy Moskovskogo mat. obschestva, 12 (1963) 3.
 41. A.N.Kolmogorov, Dokl.Akad.Nauk SSSR, 98 (1954) 527 ; General Theory of Dynamical Systems and Classical Mechanics, Proc. Int. Congress of Mathematicians, Amsterdam, 1958, Vol. I, p. 315.
 42. V.I.Arnold, Usp.Mat.Nauk, 18, No 6 (1963) 91 ; V.I.Arnold and Avez, Ergodic Problems of Classical Mechanics (Benjamin, Inc., New York, 1968).
 43. J.Moser, Nachr. Akad.Wiss., Göttingen, Math. Phys. Kl., No 1 (1962) 1 ; Stable and Random Motions in Dynamical Systems, Annals of Mathematics Studies No 77 (University Press, Princeton, 1973).
 44. V.I.Arnold, Mathematical Methods in Classical Mechanics (Nauka, Moskva, 1974) (in Russian).
 45. J.M.Greene, J.Math.Phys., 20 : 6 (1979) 1183.
 46. I.B.Vasserman, I.A.Koop, S.I.Mishnev, G.M.Tumaikin and Yu.M.Shatunov, Preprint 76-79 (Institute of Nuclear Physics, Novosibirsk, 1976).
 47. E.Keil, CERN/ISR/79-32, Geneva (1979).
 48. H.Wiedeman, SLAC-PUB-2320, PEP NOTE 299 (1979).
 49. A.W.Chao and M.Month, Nucl. Instr. and Meth. 121 (1974) 129.
 50. M.Month, Proc. IXth Int. Conf. on High Energy Acc. Stanford (1974) 402 ; IEEE Trans. NS-22, 3 (1975) 1376.
 51. A.Piwinski and A.Wrulich, Hamburg DESY-76/07 (1976).
 52. A.Piwinski, IEEE Trans. NS-24 (1977) 1408 ; DESY-77/18(1977).
 53. G.M.Zaslavsky and B.V.Chirikov, Dokl.Akad. Nauk SSSR, 159 (1964) 306.
 54. B.V.Chirikov, E.Keil and A.M.Sessler, J.Statist. Phys., 3 No 3 (1971) 307.
 55. G.Froeschlé, Astron. and Astrophys., 16 (1972) 172 ; C.Froeschlé and J.P.Scheidecker, Astron. and Astrophys., 22, (1973) 431 ; Journ. Comp. Phys. 11, No 3 (1973) 423.
 56. G.V.Gadiyak, F.M.Izrailev and B.V.Chirikov, Proc. 7-th Intern. Conf. on Nonlinear Oscillations (Berlin, 1975), Vol. II, 1, p.315.
 57. J.L.Tennyson, M.A.Liberman and A.J.Lichtenberg, "Diffusion in Near-Integrable Hamiltonian Systems with Three Degrees

of Freedom", AIP Conf., Proc. of "Symposium on Nonlinear Dynamics and Beam-Beam Interaction", Brookhaven Nat. Lab., March 19-21 (1979) 272.

58. B.V.Chirikov, J.Ford and F.Vivaldi, "Some Numerical Studies of Arnold Diffusion in a Simple Model", AIP Conf., Proc. of "Symposium on Nonlinear Dynamics and Beam-Beam Interaction, Brookhaven Nat.Lab., March 19-21 (1979) 323.
59. I.B.Vasserman, F.M.Izrailev and G.M.Tumaikin, Preprint 79-74 (Institute of Nuclear Physics, Novosibirsk, 1979).
60. J.Ford and G.H.Lunsford, Phys. Rev. A1 (1970) 59.

Работа поступила - 8 января 1980 г.

Ответственный за выпуск - С.Г.Попов
Подписано к печати 3.У1-1980г. МН 07153
Усл. 3,0 печ.л., 2,9 учетно-изд.л.
Тираж 290 экз. Бесплатно
Заказ № 149.

Отпечатано на ротапинтере ИЯФ СО АН СССР